Figures

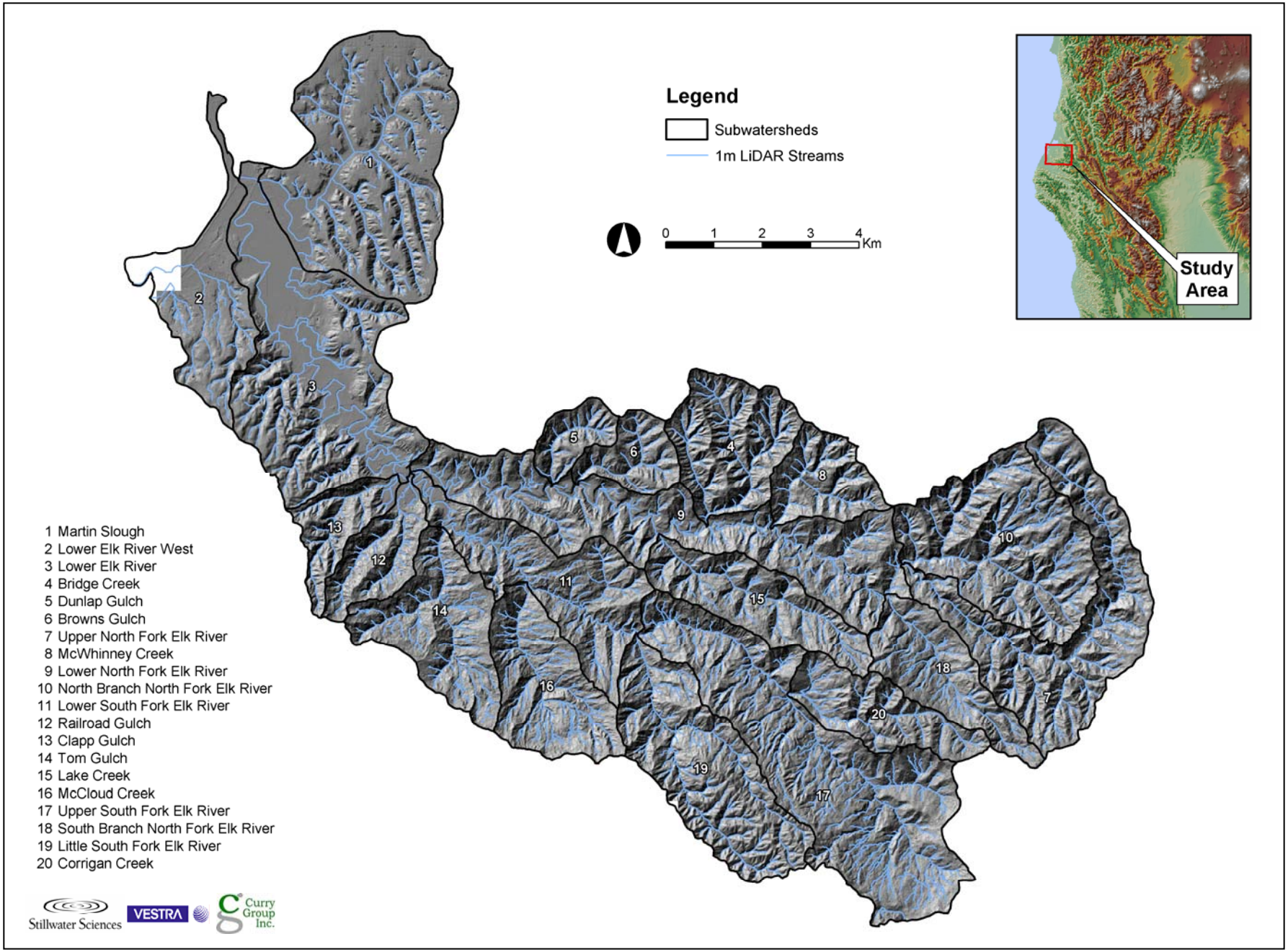

Figure 1-1. Elk River basin and subwatesheds.

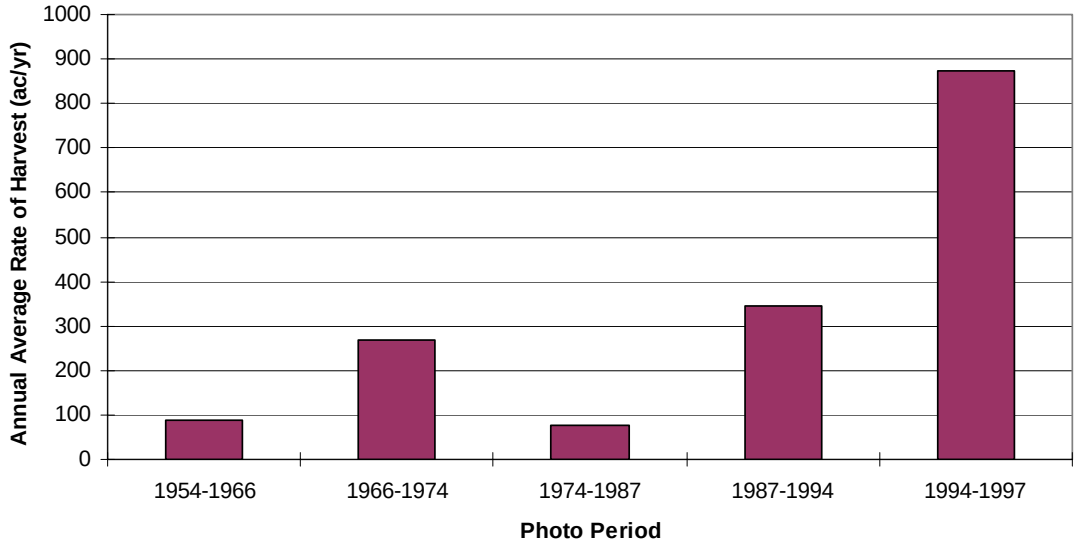

Figure 1-2. Annual average harvest rate for available photo periods in North Fork Elk River.

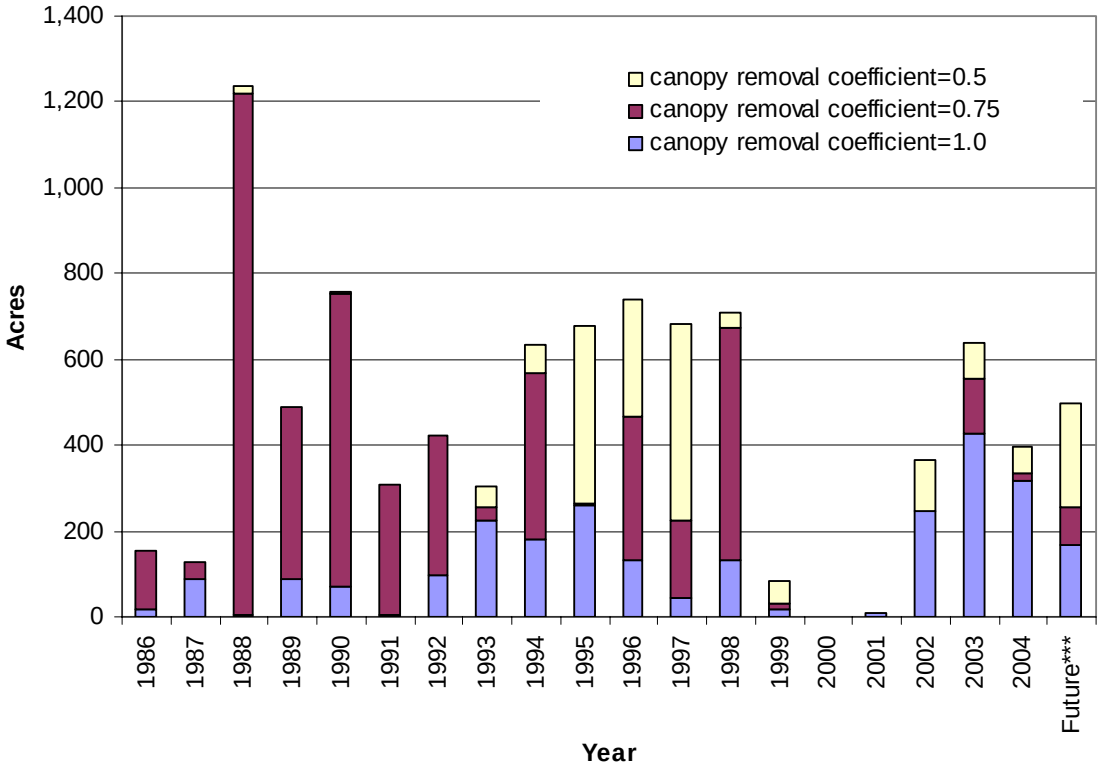

Figure 1-3. Annual harvest acreage for North Fork Elk River (all ownerships) as expressed in clear-cut equivalent acres (canopy removal coefficient of 1.0 for clear cutting, 0.75 for intermediate steps, and 0.5 for selection and commercial thin).

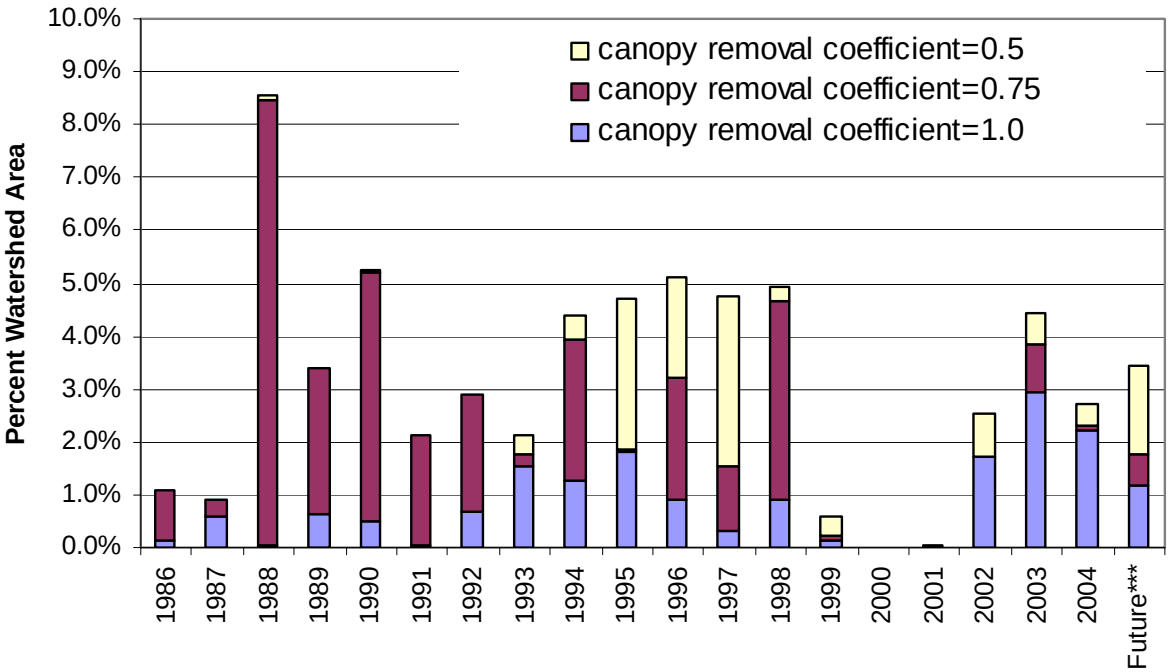

Figure 1-4. Percent of watershed harvest annually for North Fork Elk River (all ownerships) as expressed in clear-cut equivalent acres (canopy removal coefficient of 1.0 for clear cutting, 0.75 for intermediate steps, and 0.5 for selection and commercial thin).

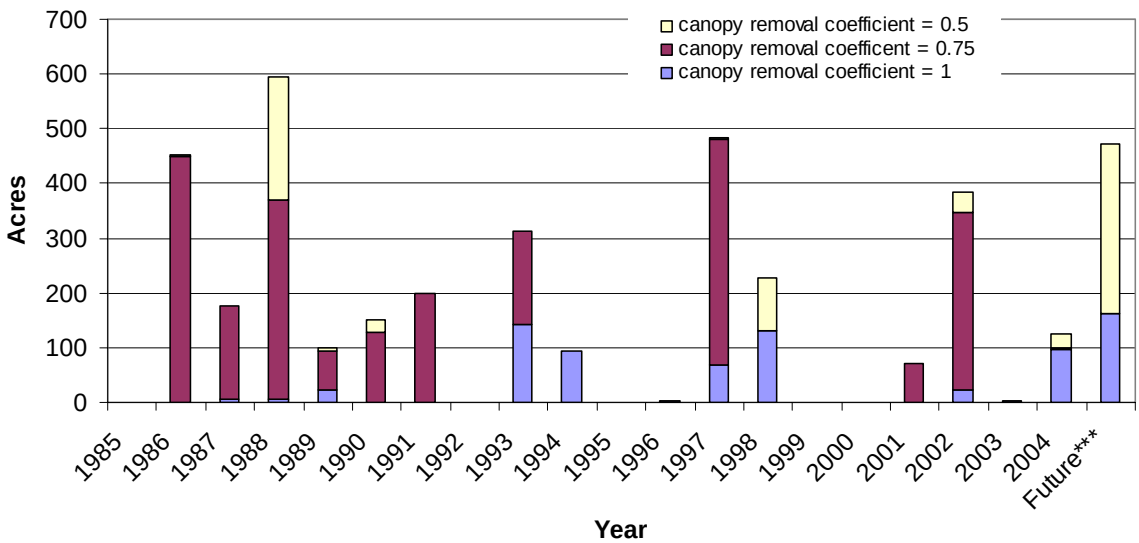

Figure 1-5. Annual harvest acreage for South Fork Elk River (all ownerships) as expressed in clear-cut equivalent acres (canopy removal coefficient of 1.0 for clear cutting, 0.75 for intermediate steps, and 0.5 for selection and commercial thin).

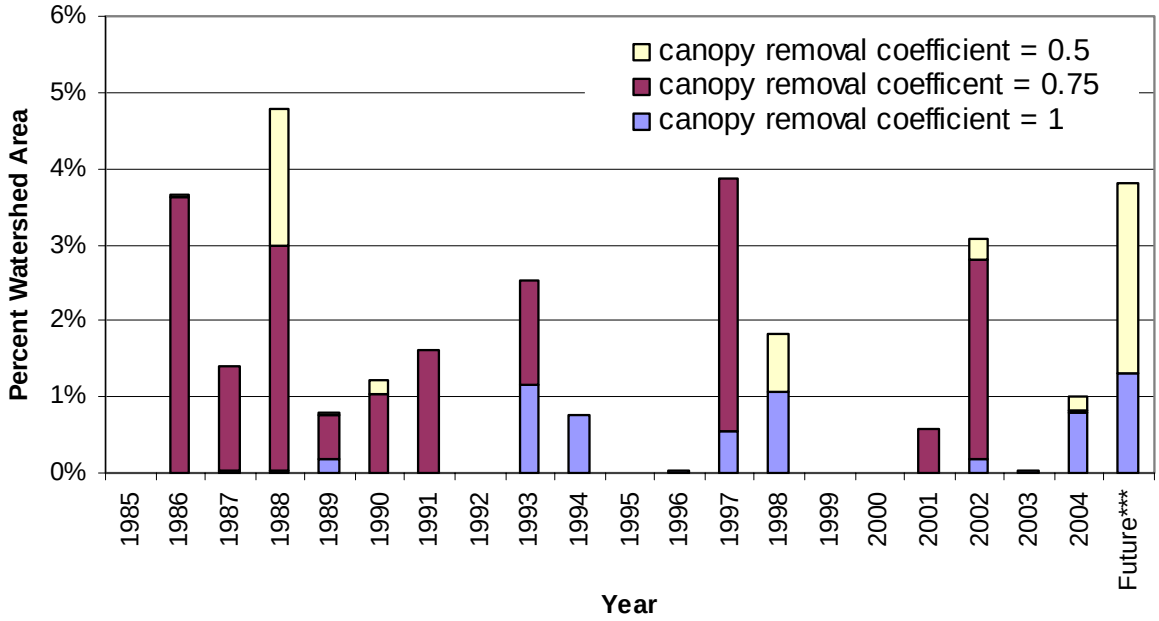

Figure 1-6. Percent of watershed harvest annually for South Fork Elk River (all ownerships) as expressed in clear-cut equivalent acres (canopy removal coefficient of 1.0 for clear cutting, 0.75 for intermediate steps, and 0.5 for selection and commercial thin).

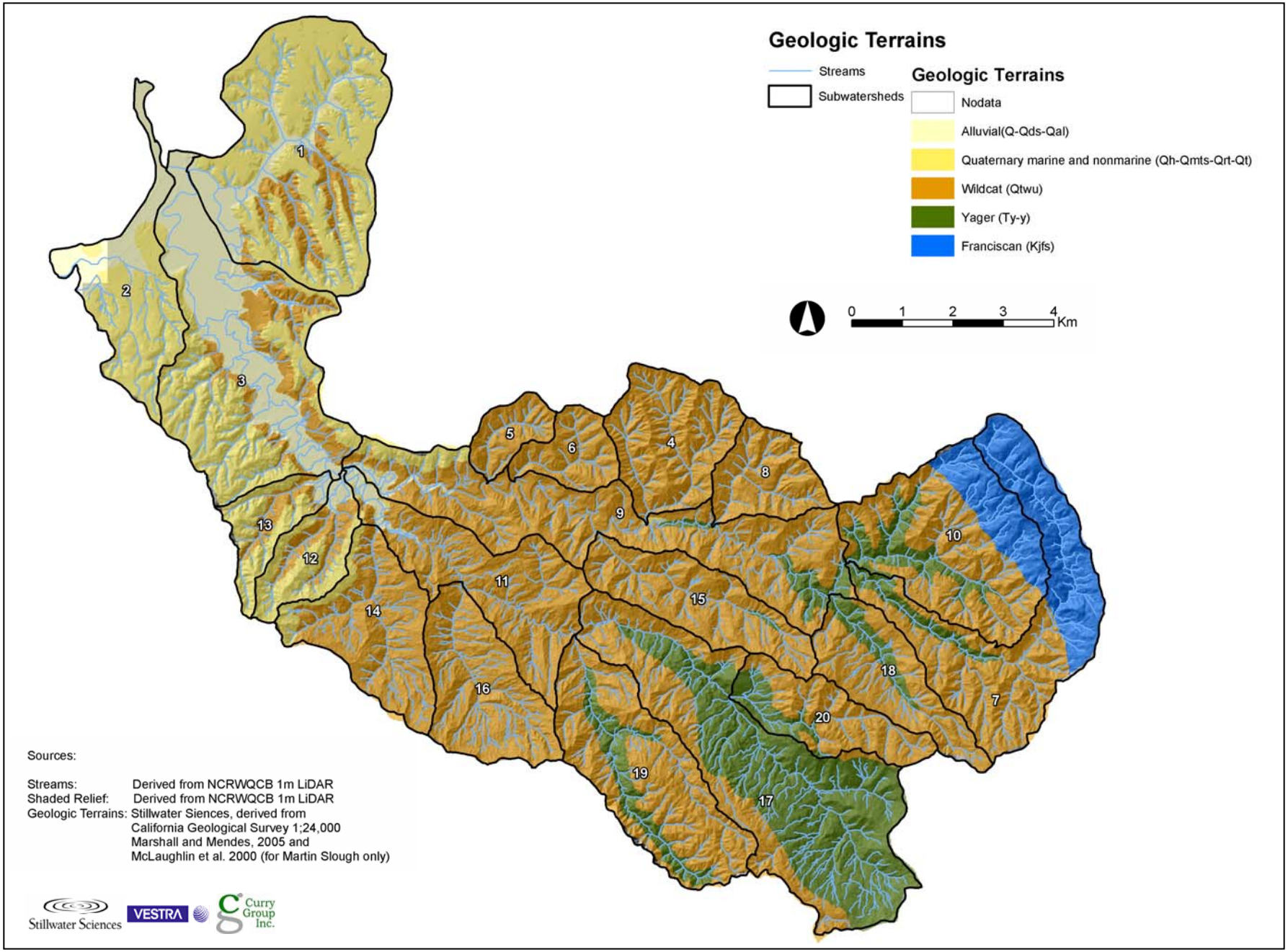

Figure 2-1. Geology in the Elk River basin (modified from McLaughlin et al. 2000, Marshall and Mendes 2005).

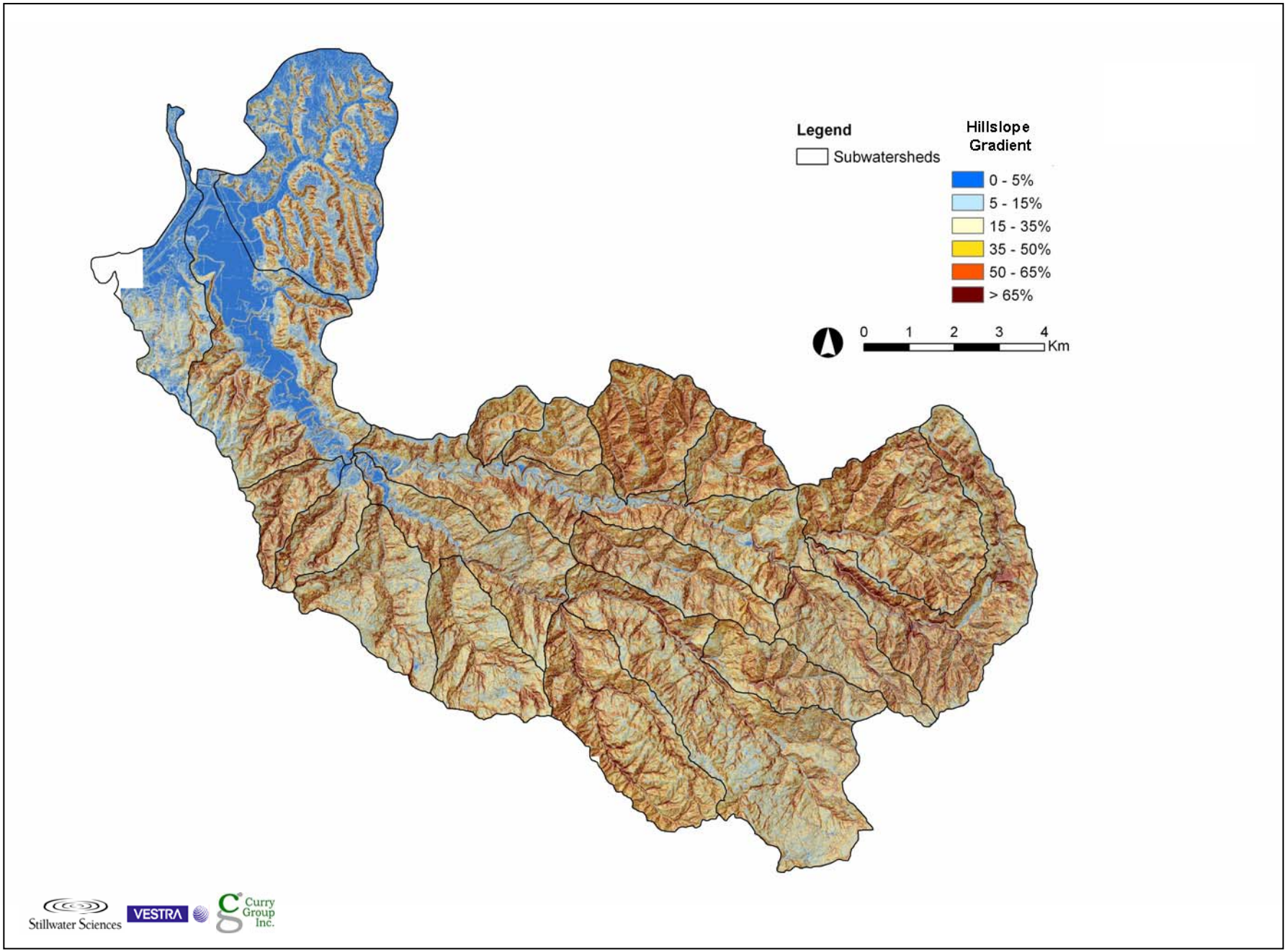

Figure 2-2. Hillslope gradient in the Elk River basin (derived from 1-m LiDAR DEM).

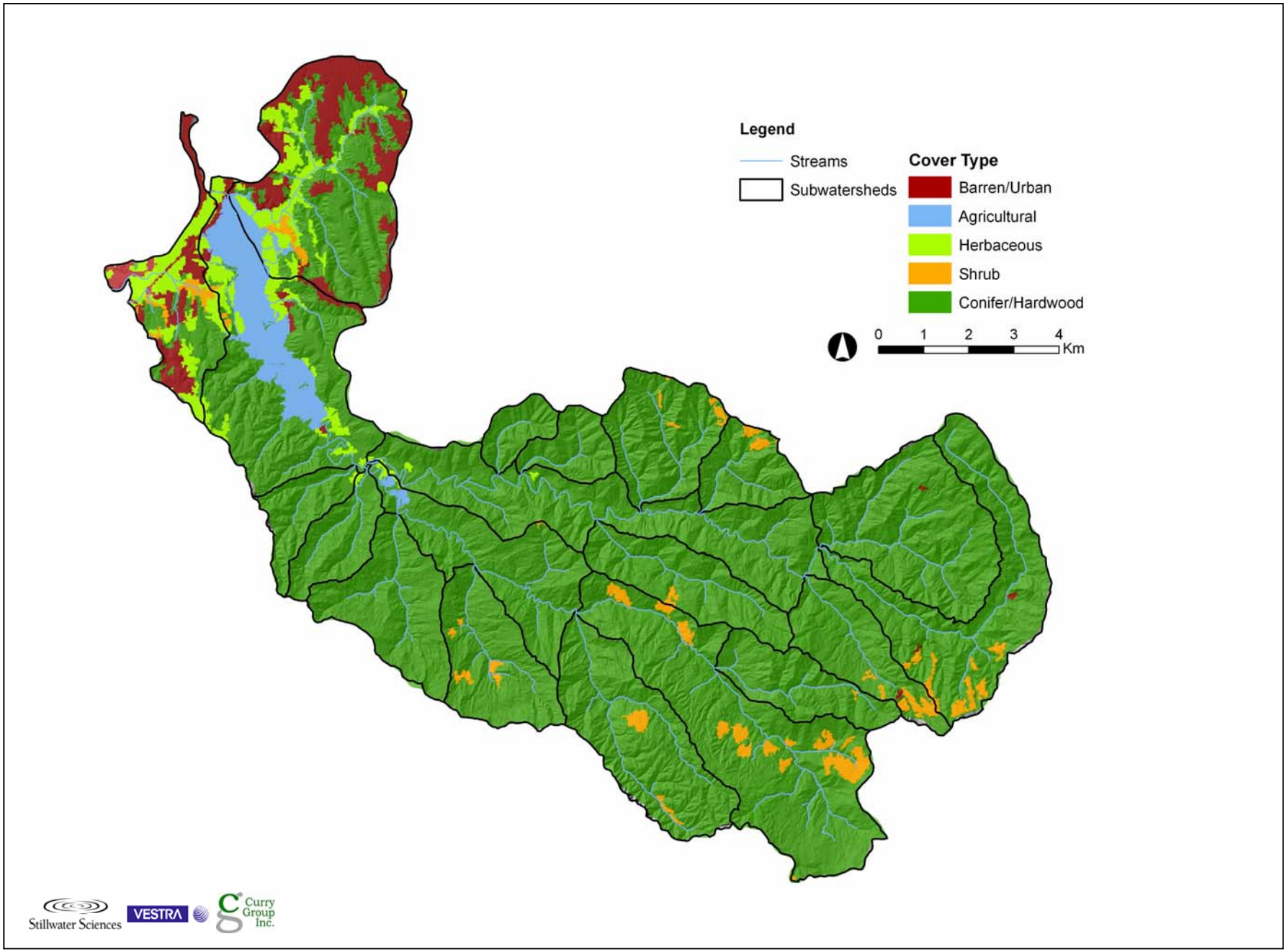

Figure 2-3. Cover type in the Elk River basin (modified from CDF-LCMMP vegetation mapping).

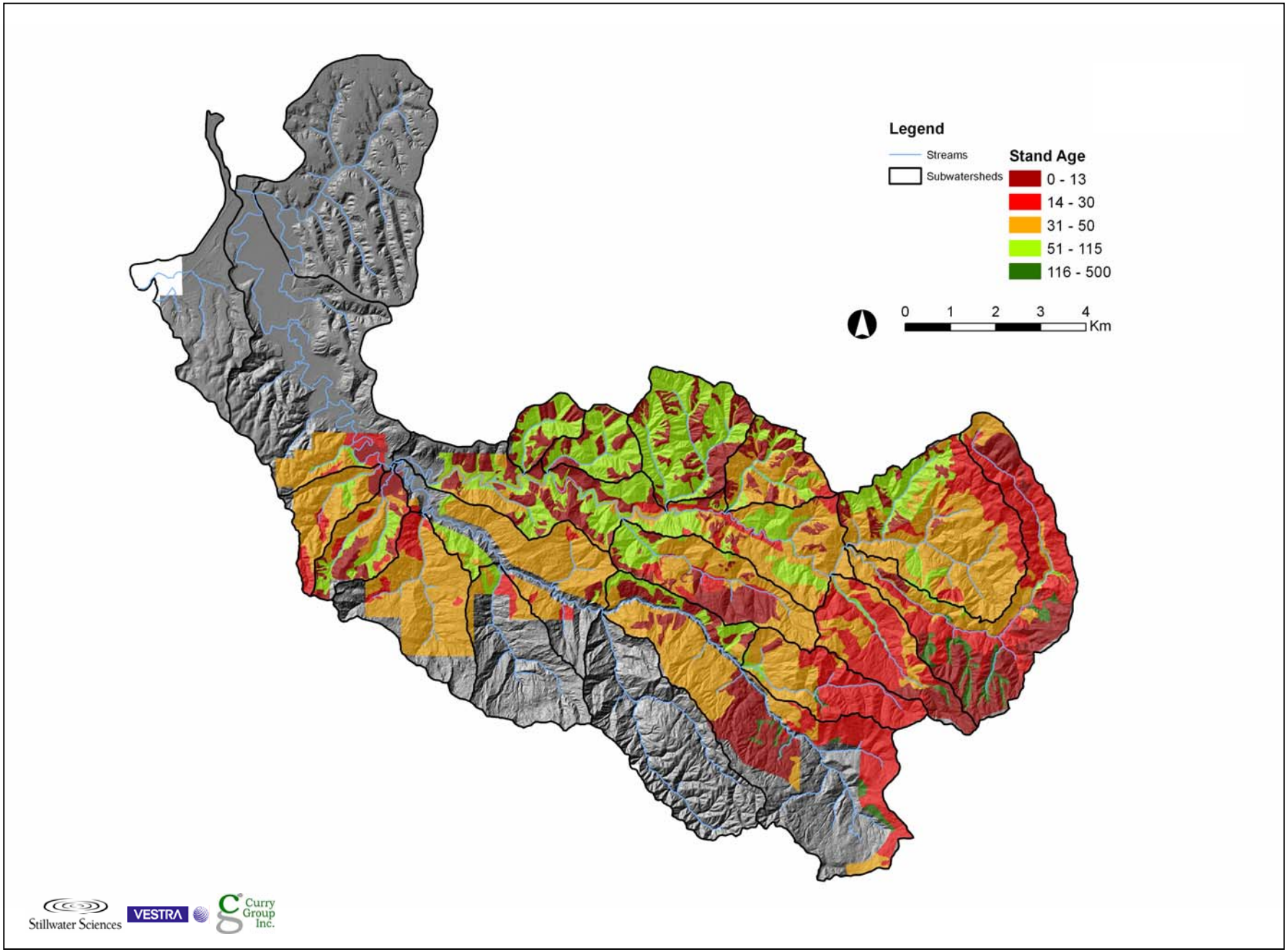

Figure 2-4. Stand age in portions of the Elk River basin (derived from PALCO stand age coverage).

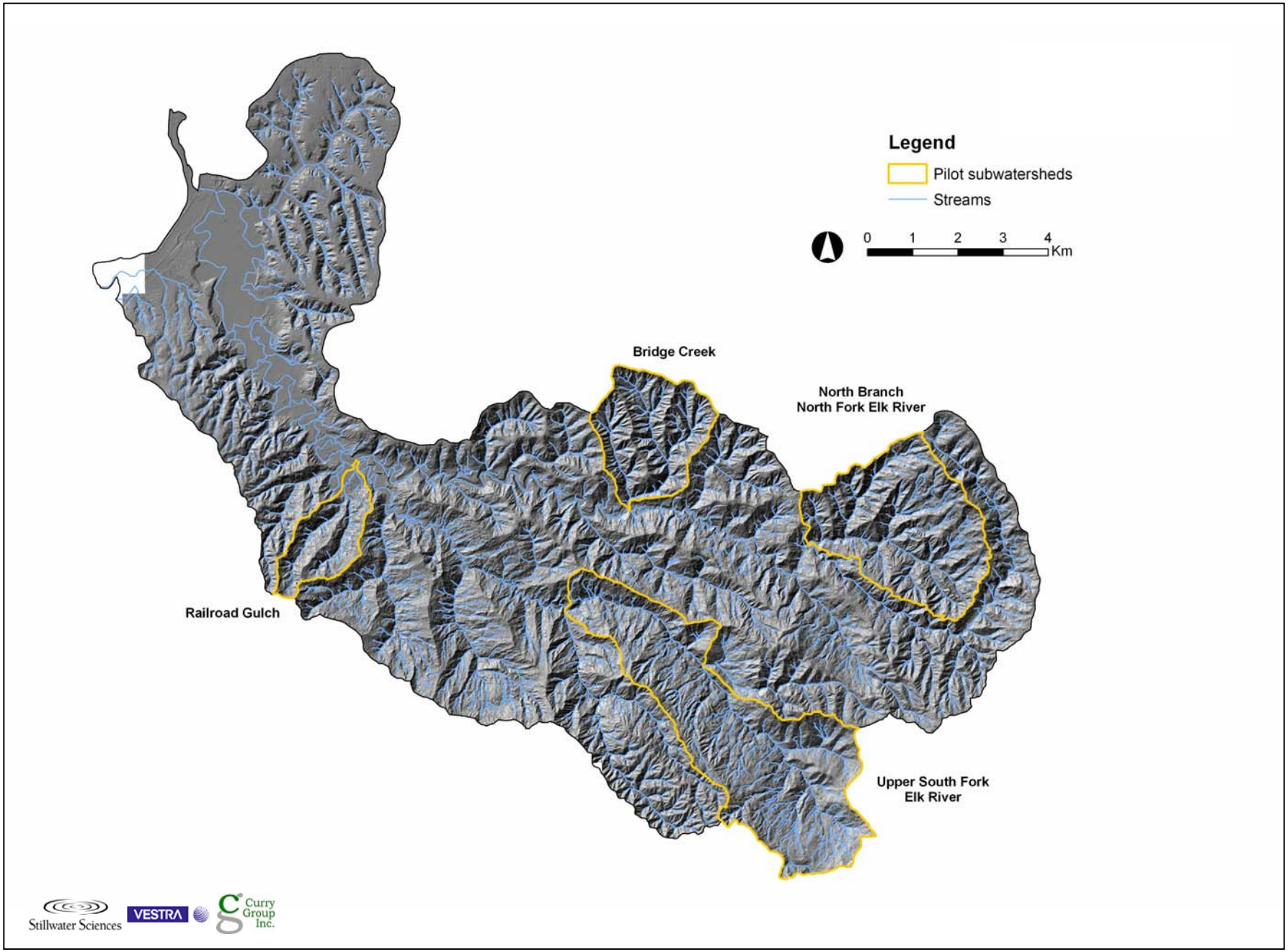

Figure 2-5. Pilot subwatersheds in the Elk River basin.

kriged 1-m DEM
Spherical semivariogram model, 8 points, 20-m radius

TIN-lattice 1-m DEM
Bilinear interpolation among 4 cells

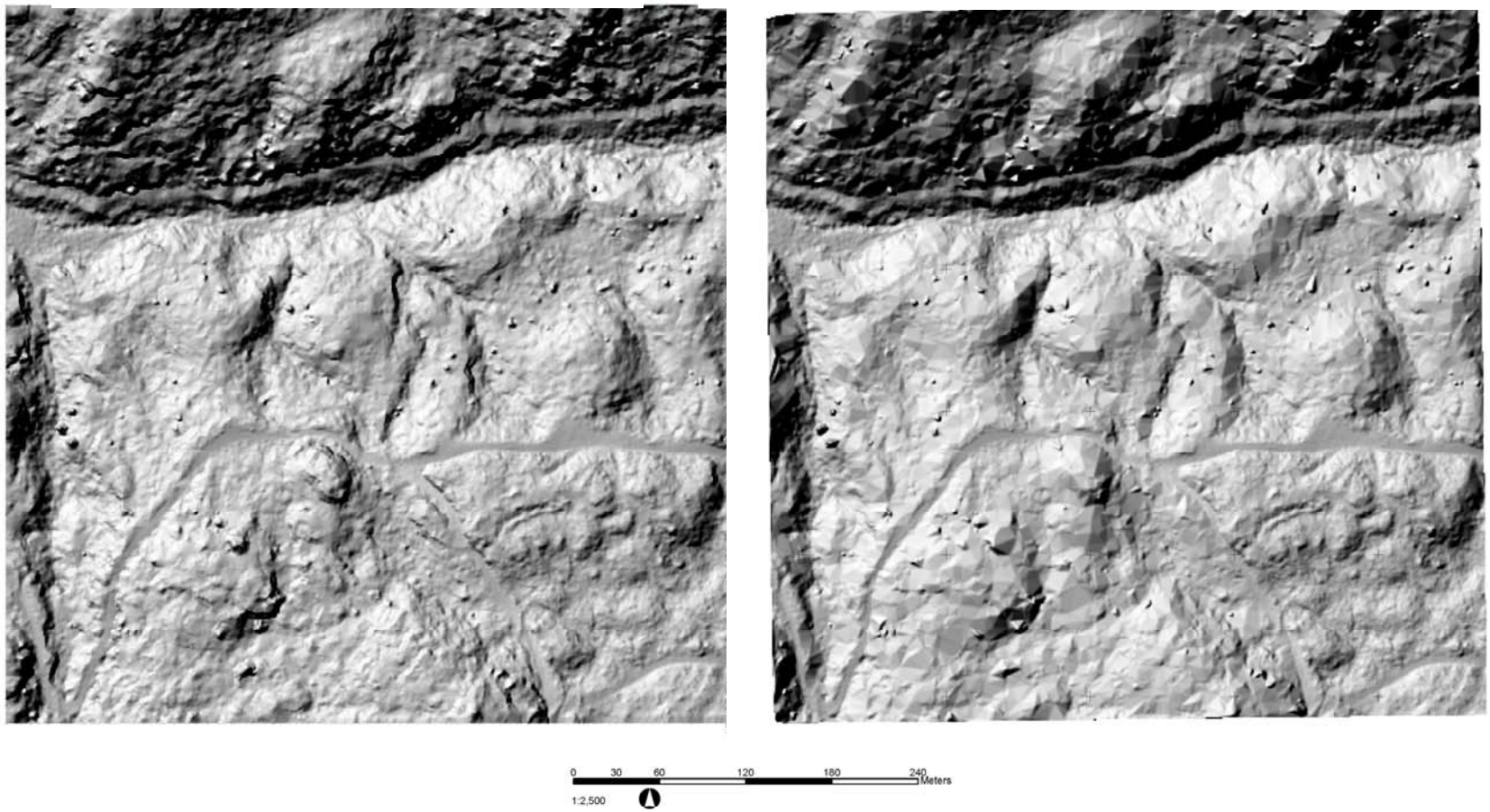

Figure 2-6. Comparison of hillshade images from 1-m grids created from TINing and Kriging methods.

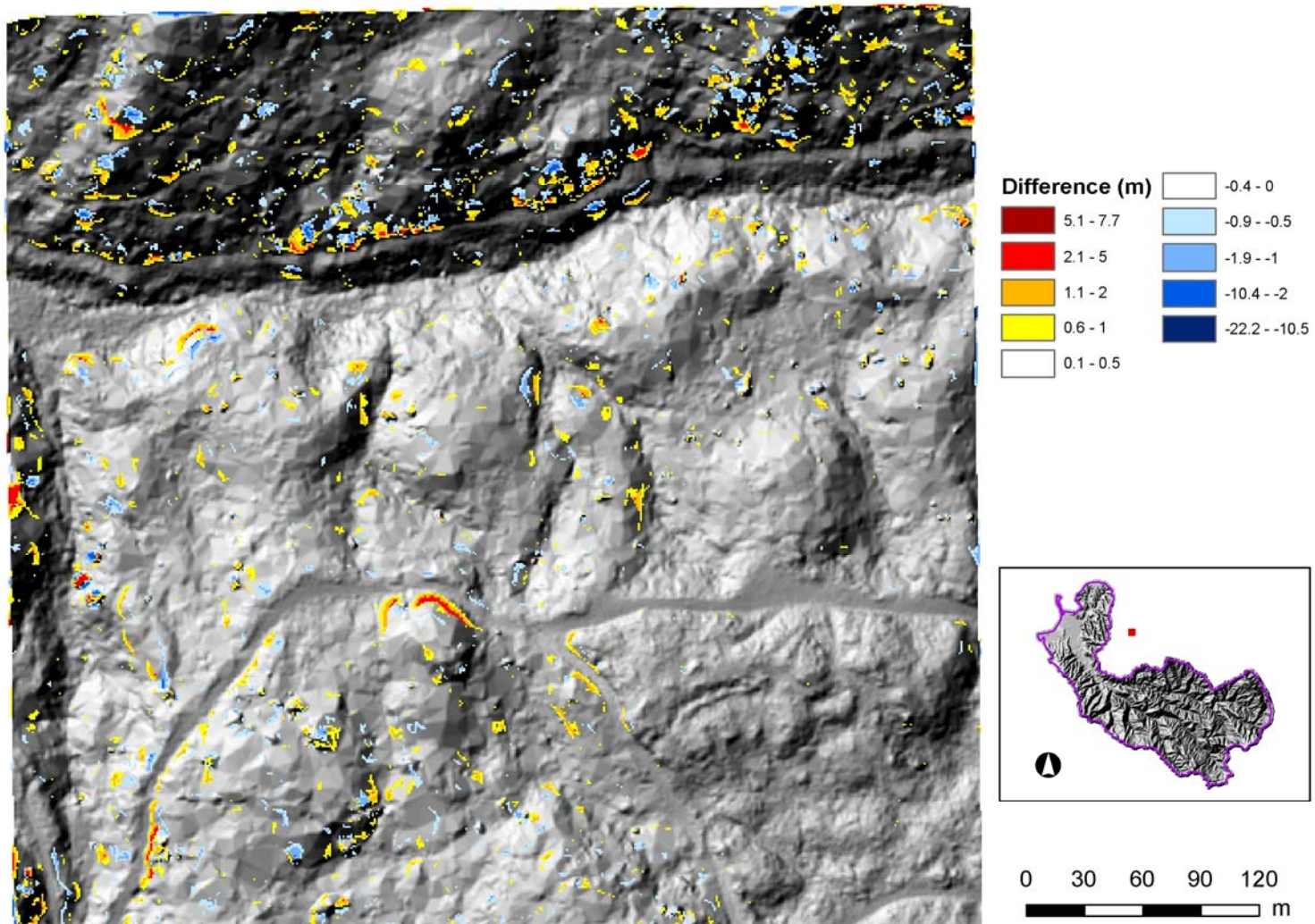

Figure 2-7. Elevation differences between 1-m grids created by TINing and Kriging methods.

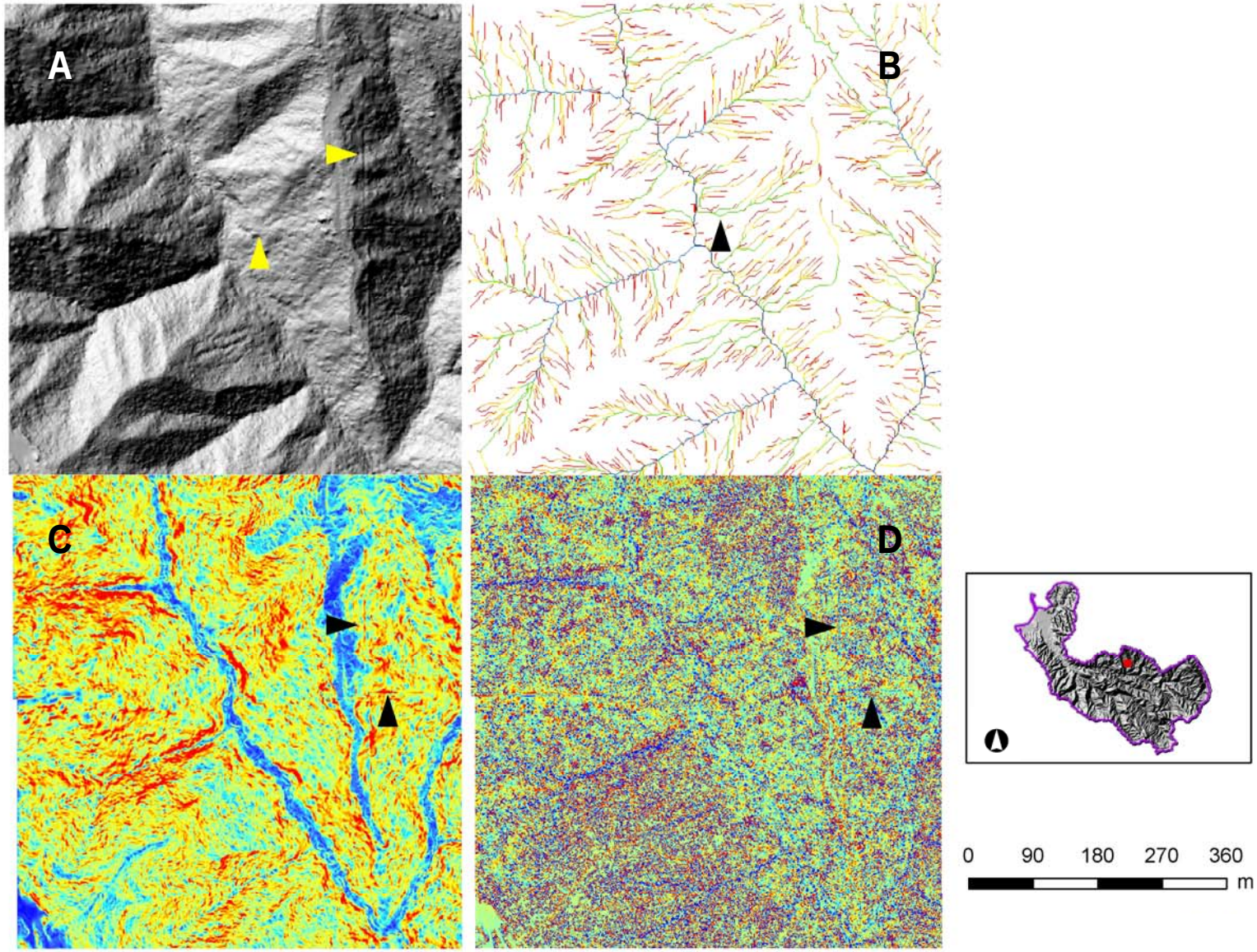

Figure 2-8. Tiling artifacts from the initial 1-m grid created by kriging (spherical semivariogram, search raddius 20, maximum of 16 points)(Sanborn 2005). A) shaded relief, B) flow accumulation, C) hillslope gradient, D) curvature.

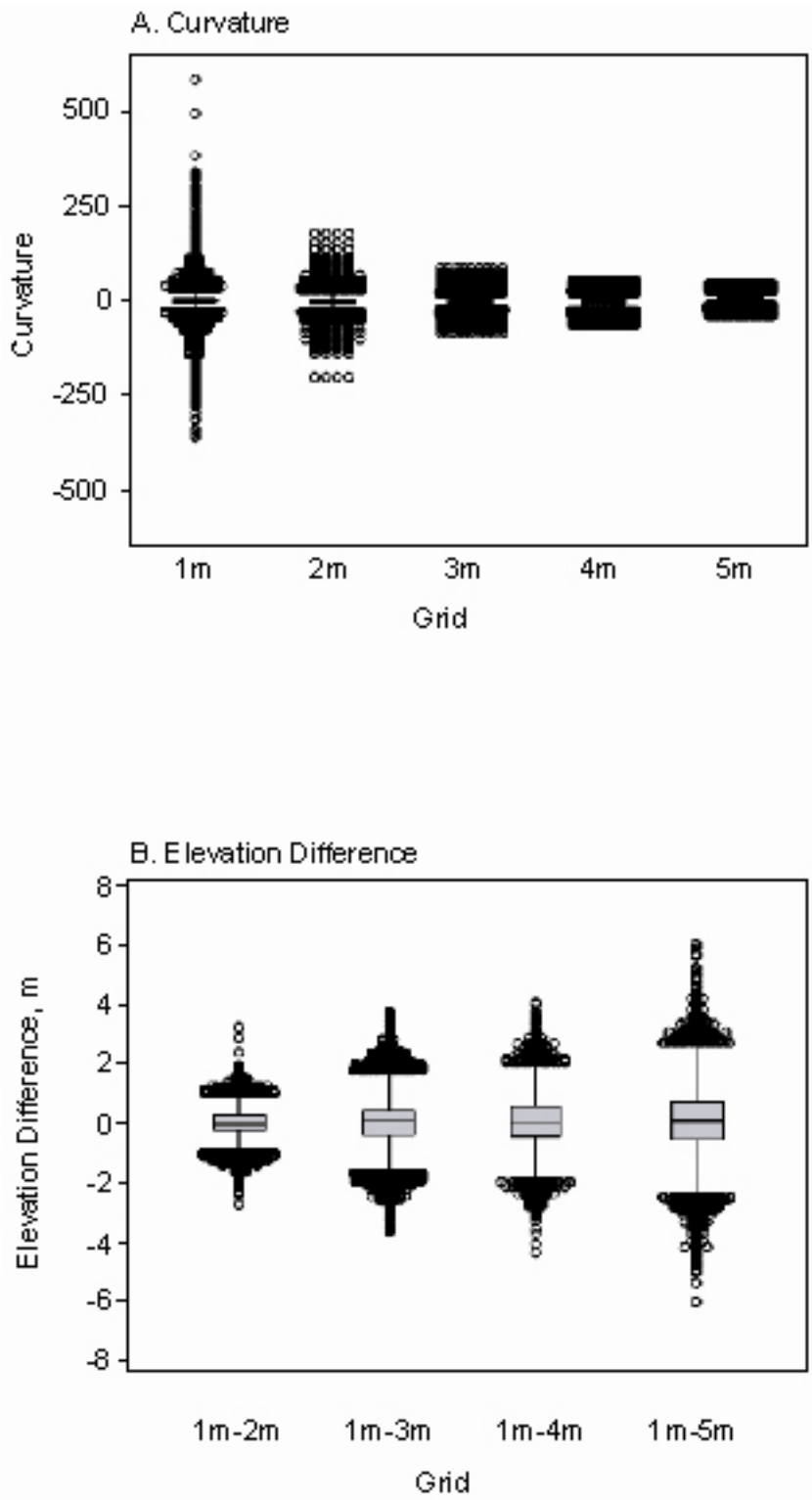

Figure 2-9. Comparison of curvature and elevation changes for different DEM grid sizes.

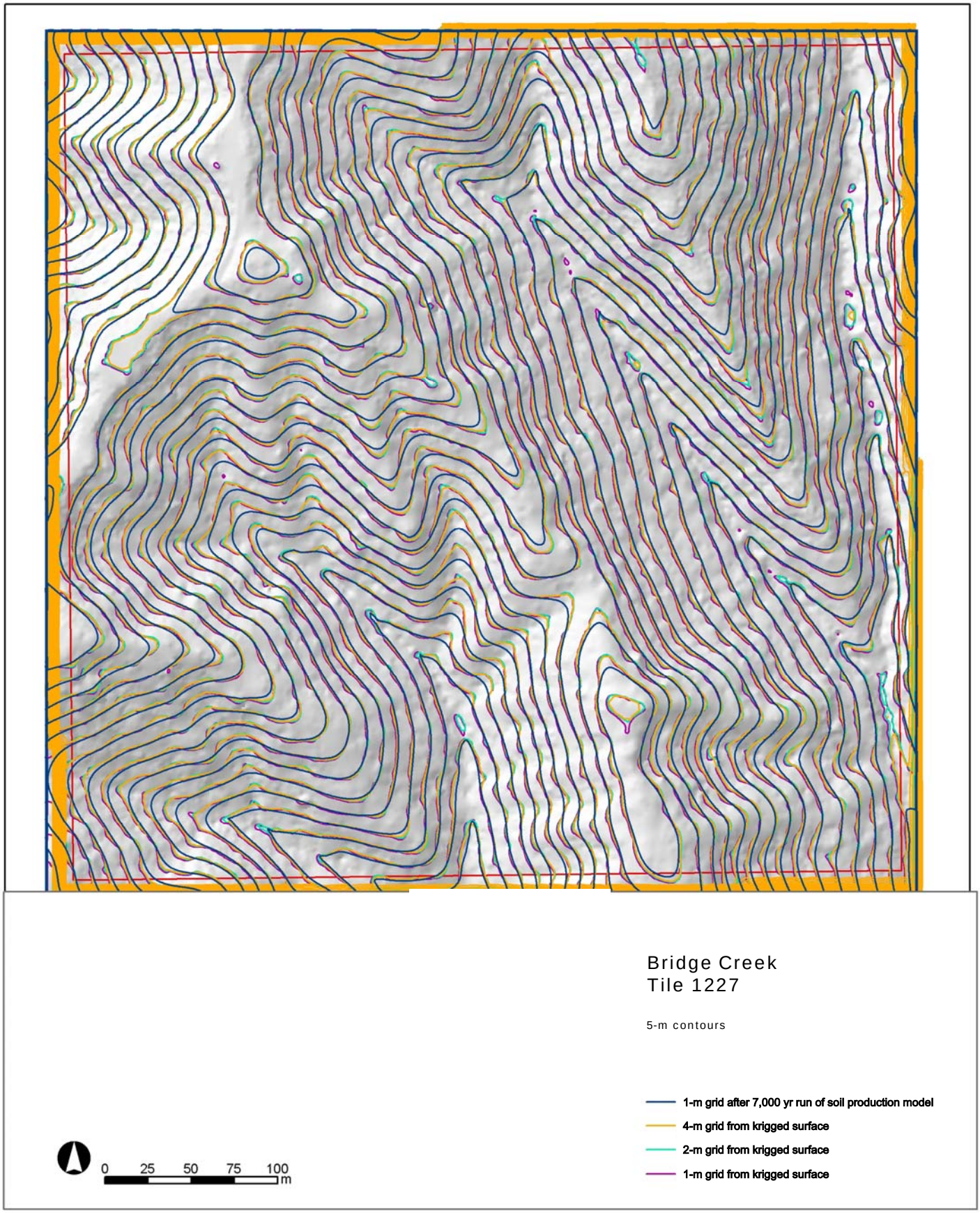

Figure 2-10. Comparison of contours generated from different DEM grid sizes and methods.

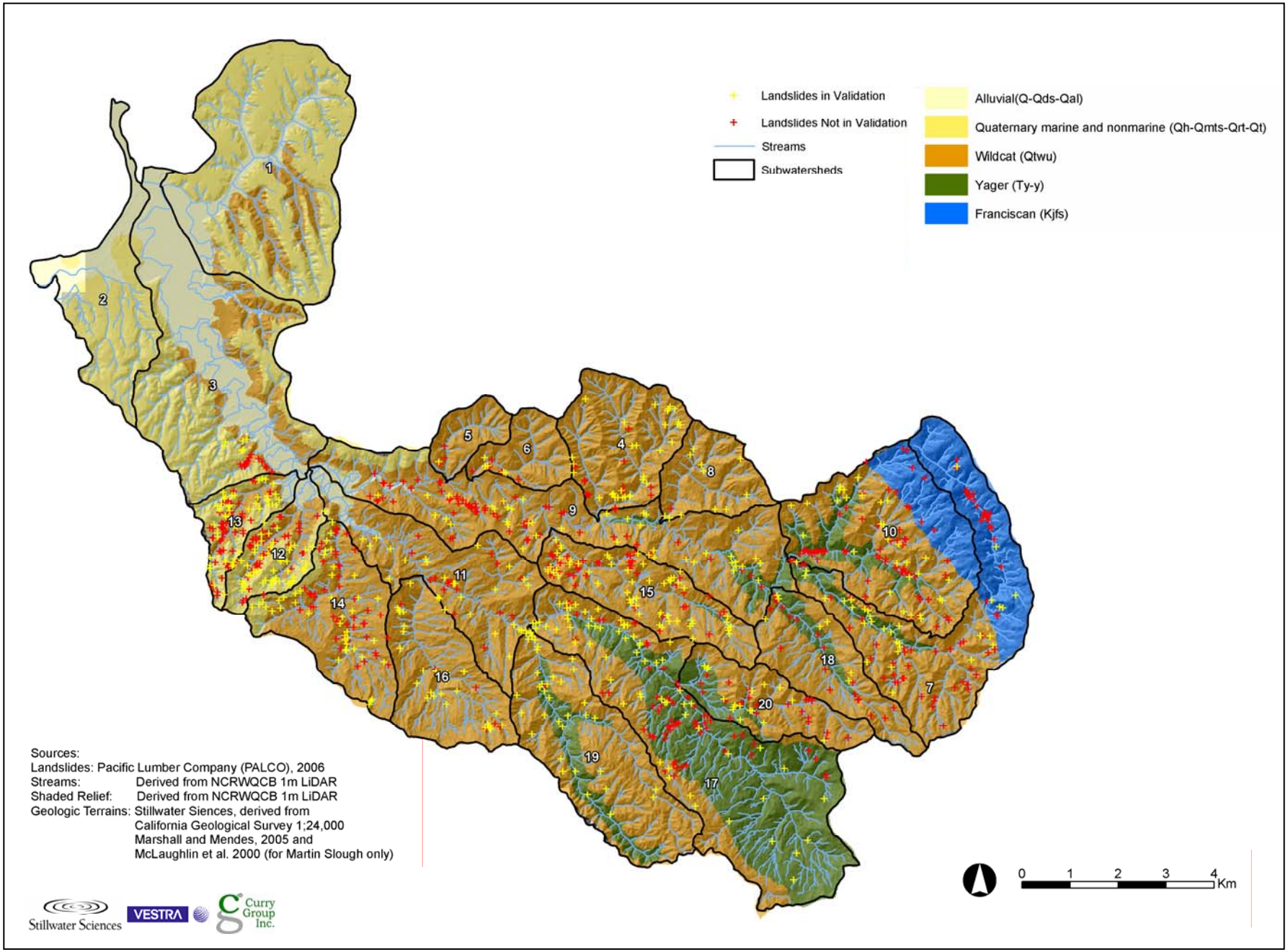

Figure 2-11. Composite shallow landslide data for model testing in the Elk River basin.

Figure 3-1. SHALSTAB results in the Elk River basin.

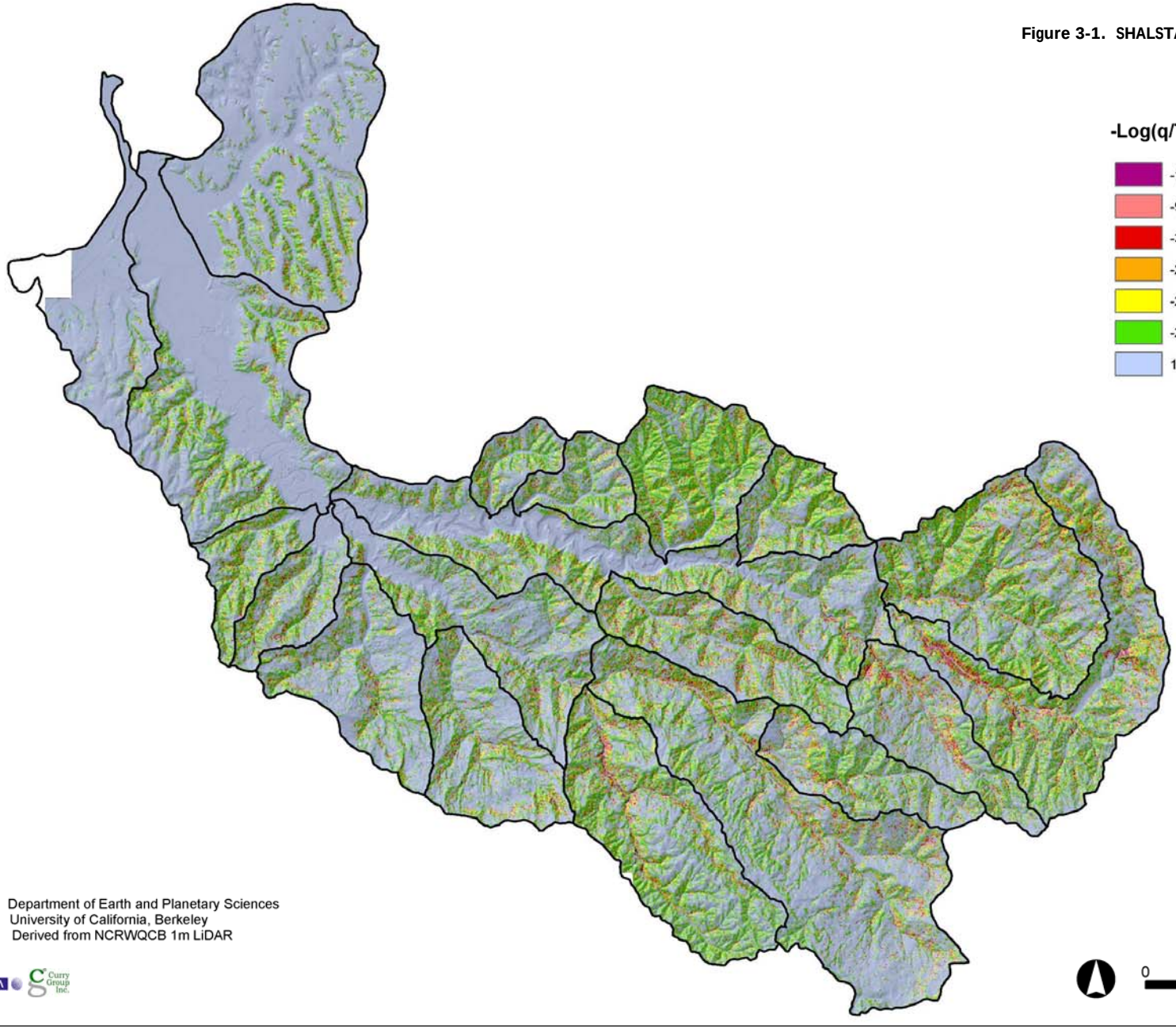

Figure 3-2. SHALSTAB V results in the Elk River basin.

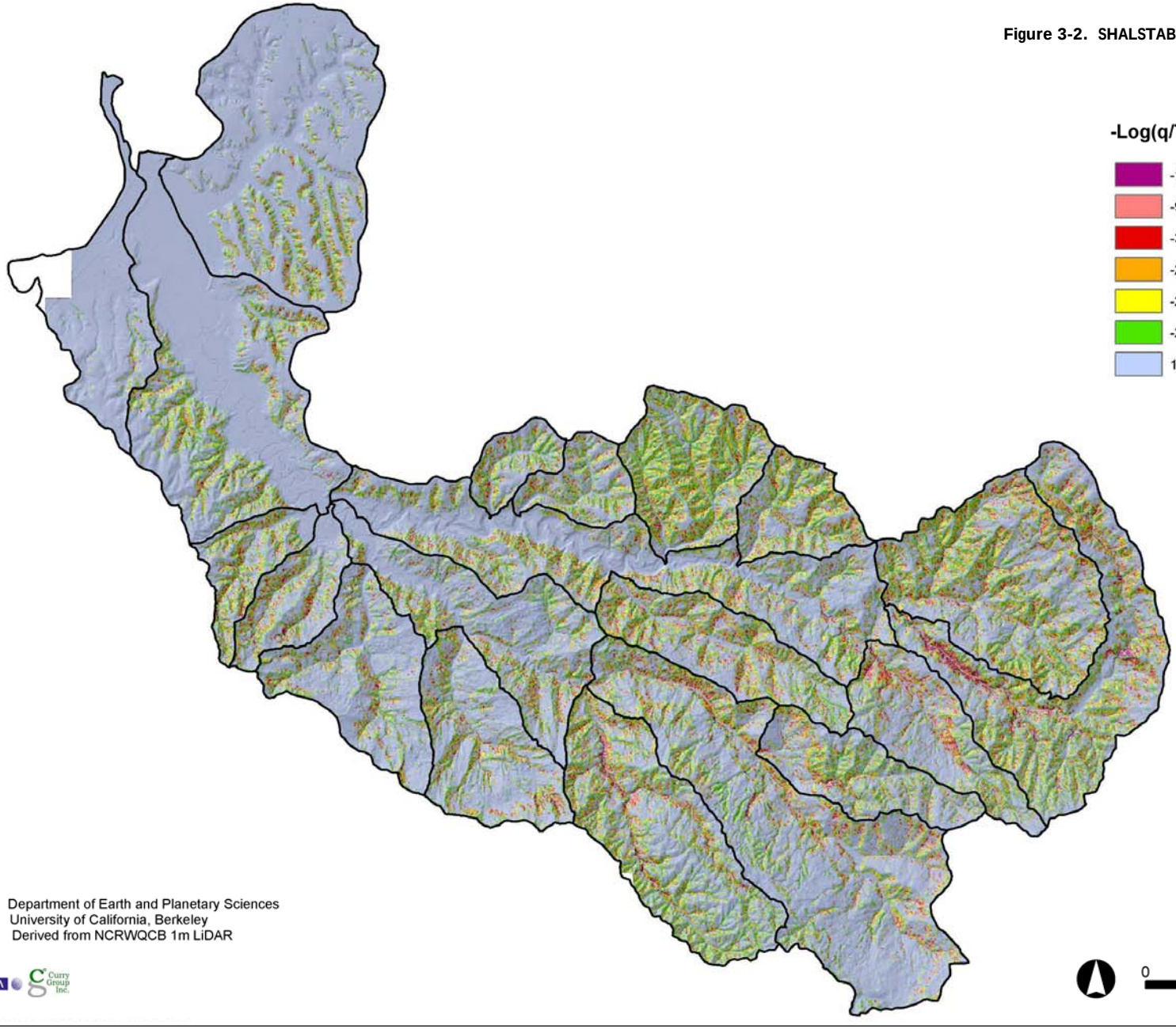

Figure 3-3. PISA results in the Elk River basin.

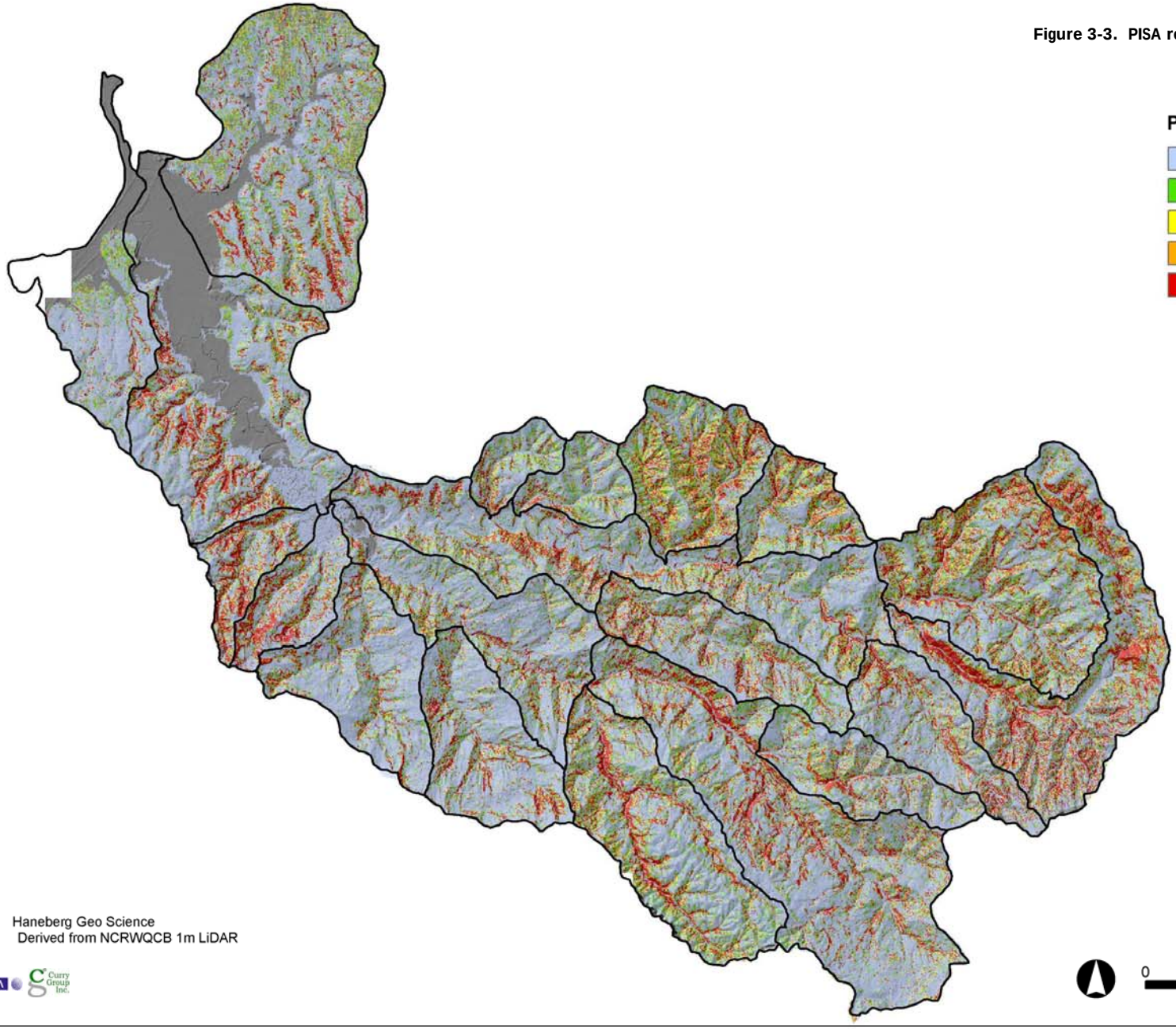

Figure 3-4. PISA.V results in the Elk River basin.

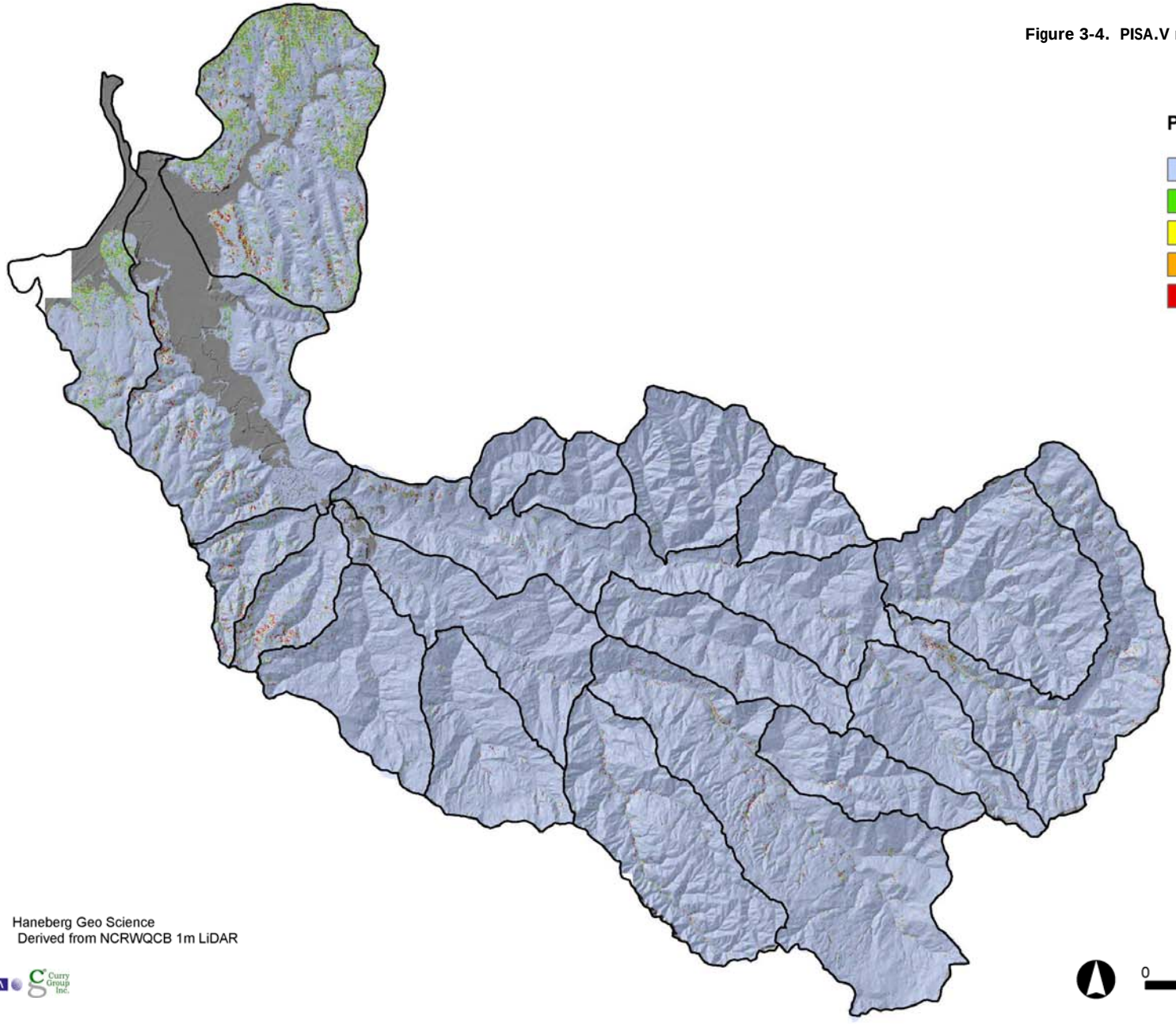

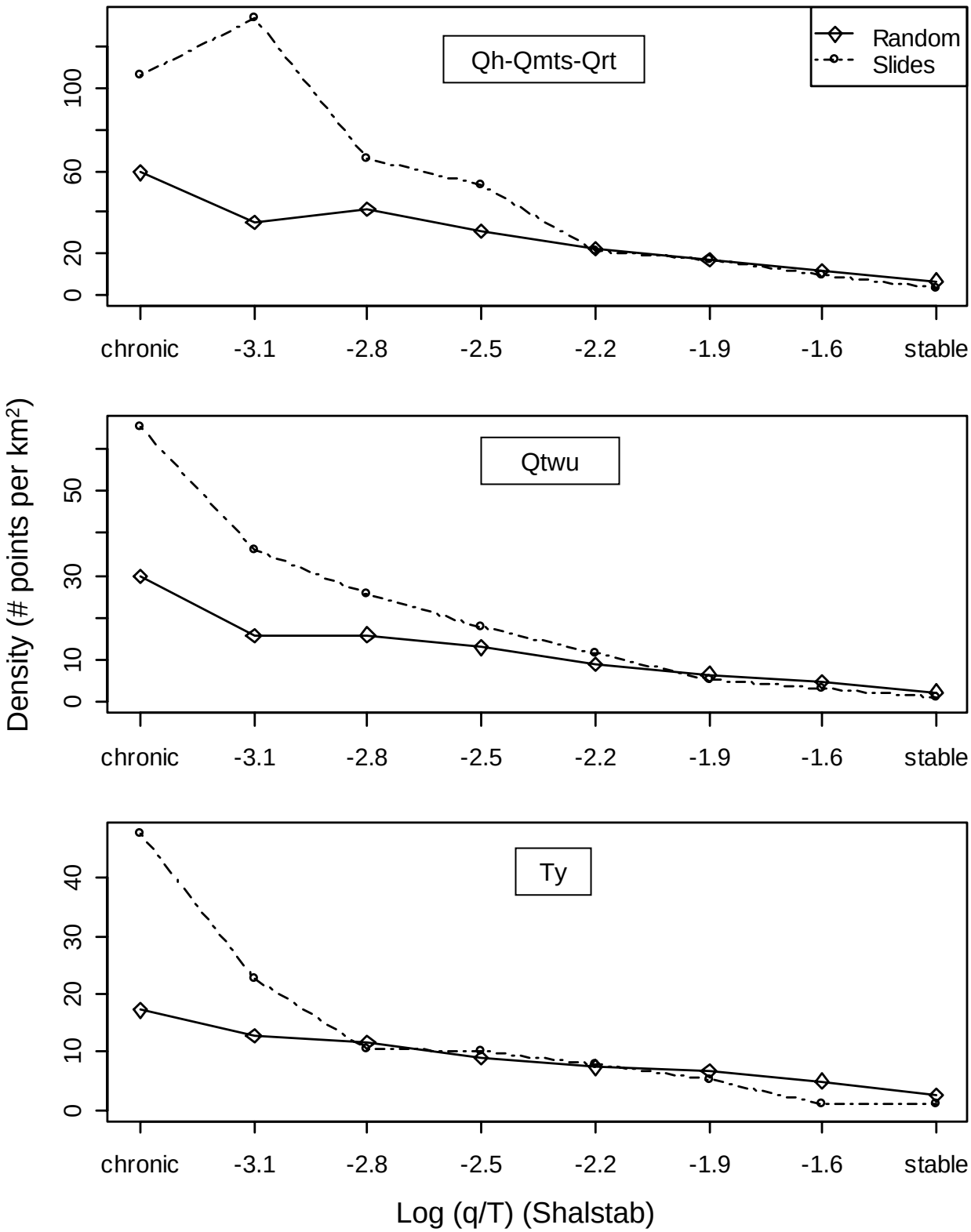

Figure 3-5. Density of landslides and random points by log (q/T) class from SHALSTAB.

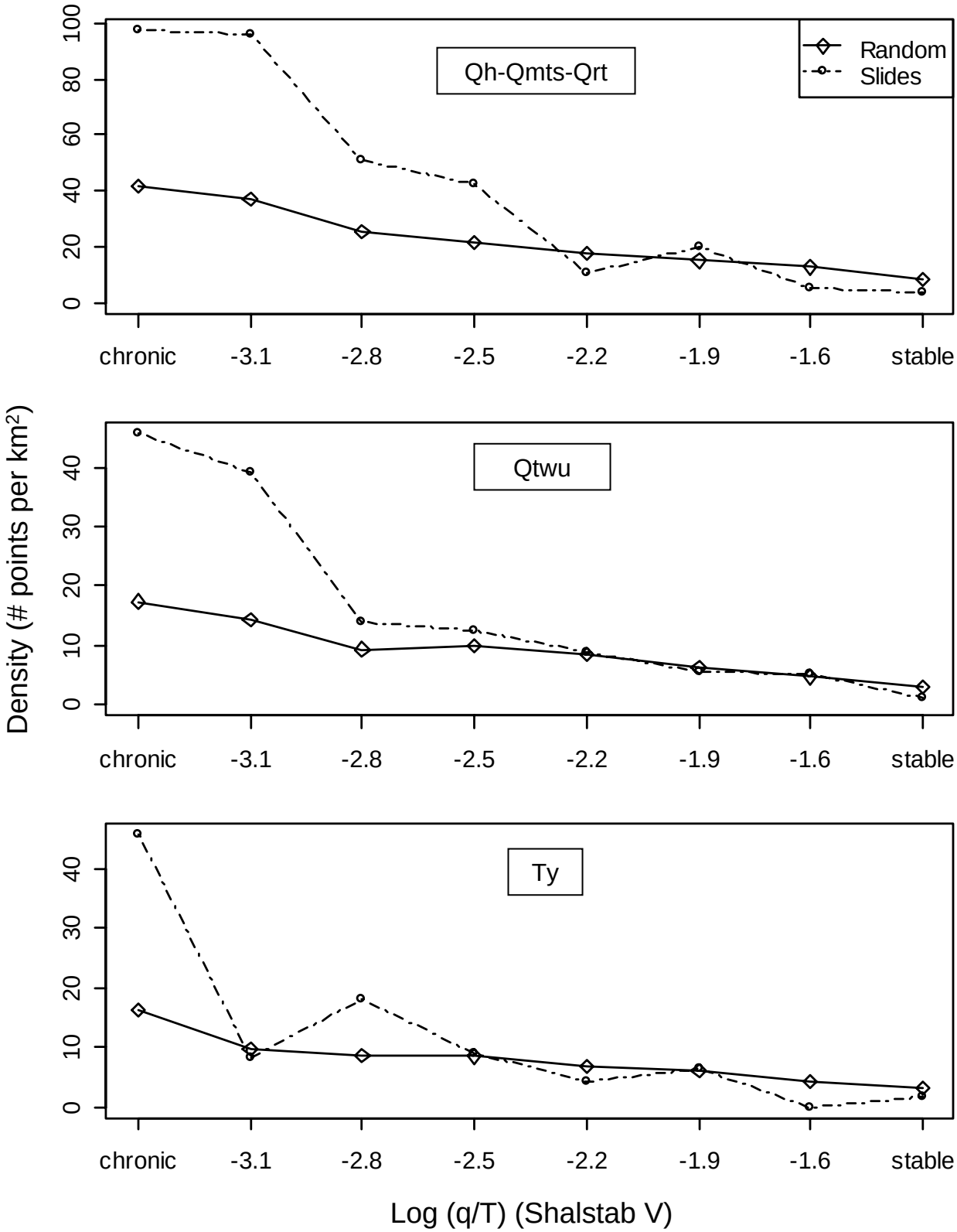

Figure 3-6. Density of landslides and random points by log (q/T) class from SHALSTAB.V.

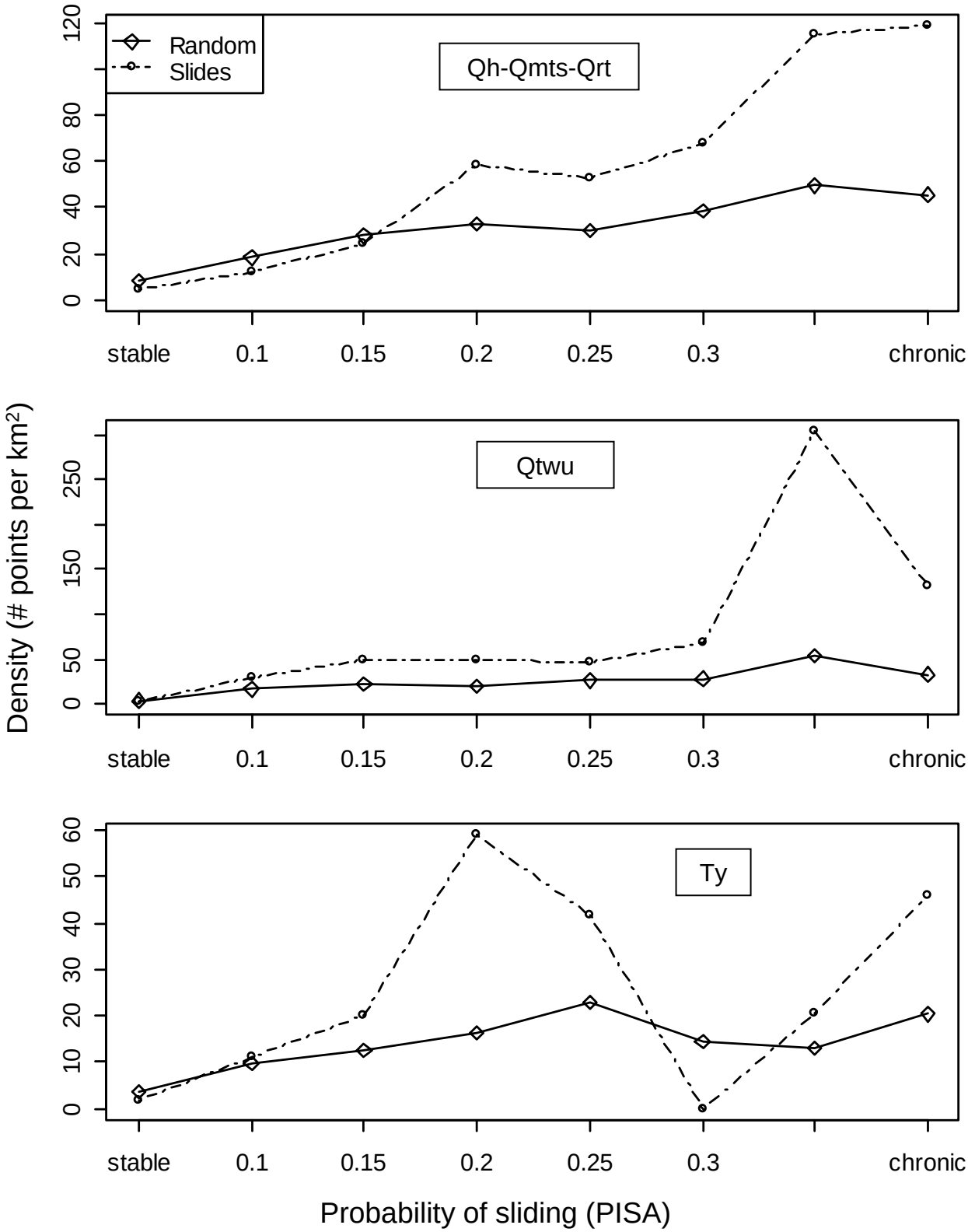

Figure 3-7. Density of landslides and random points by probability of sliding from PISA.

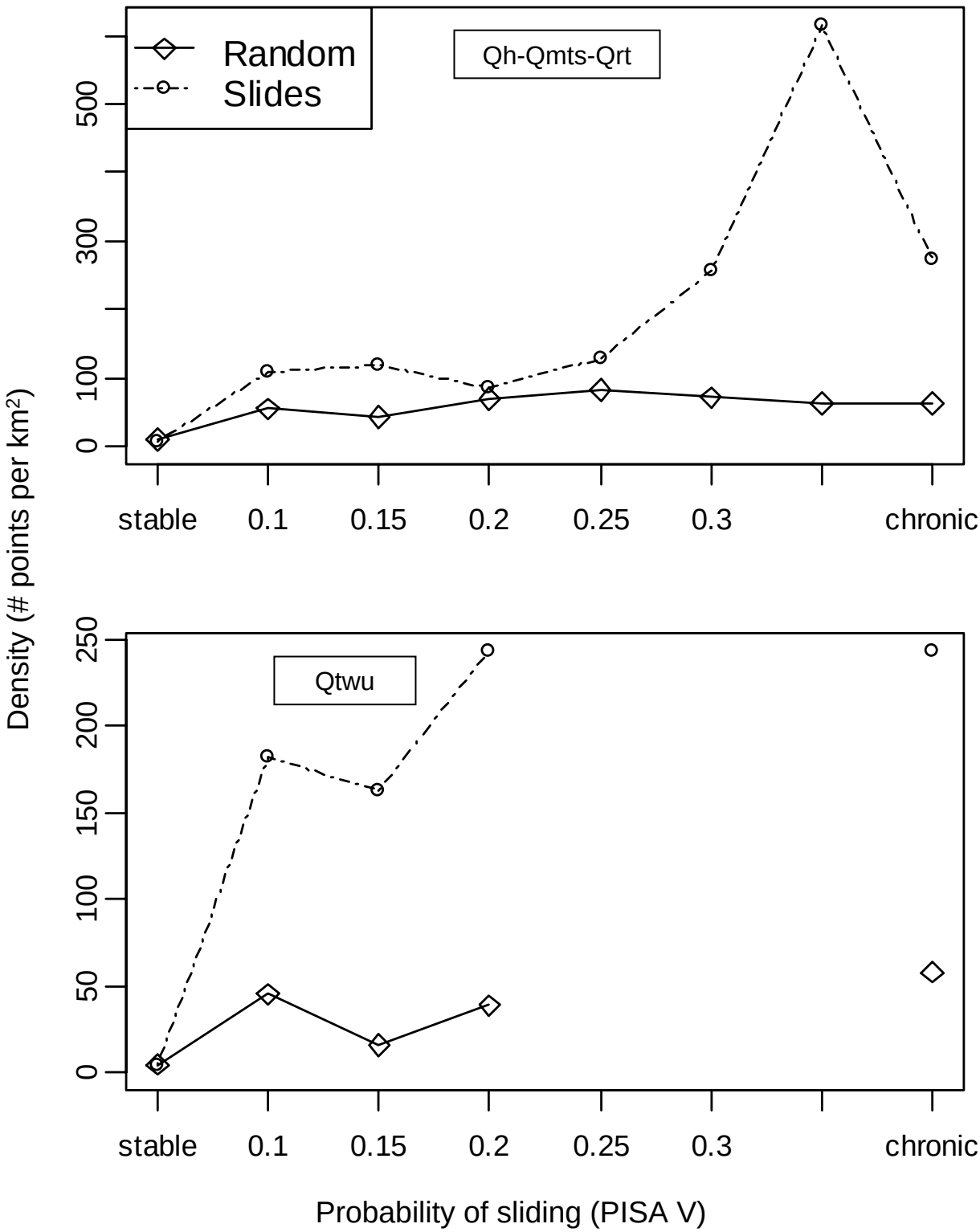

Figure 3-8. Density of landslides and random points by probability of sliding from PISA.V.

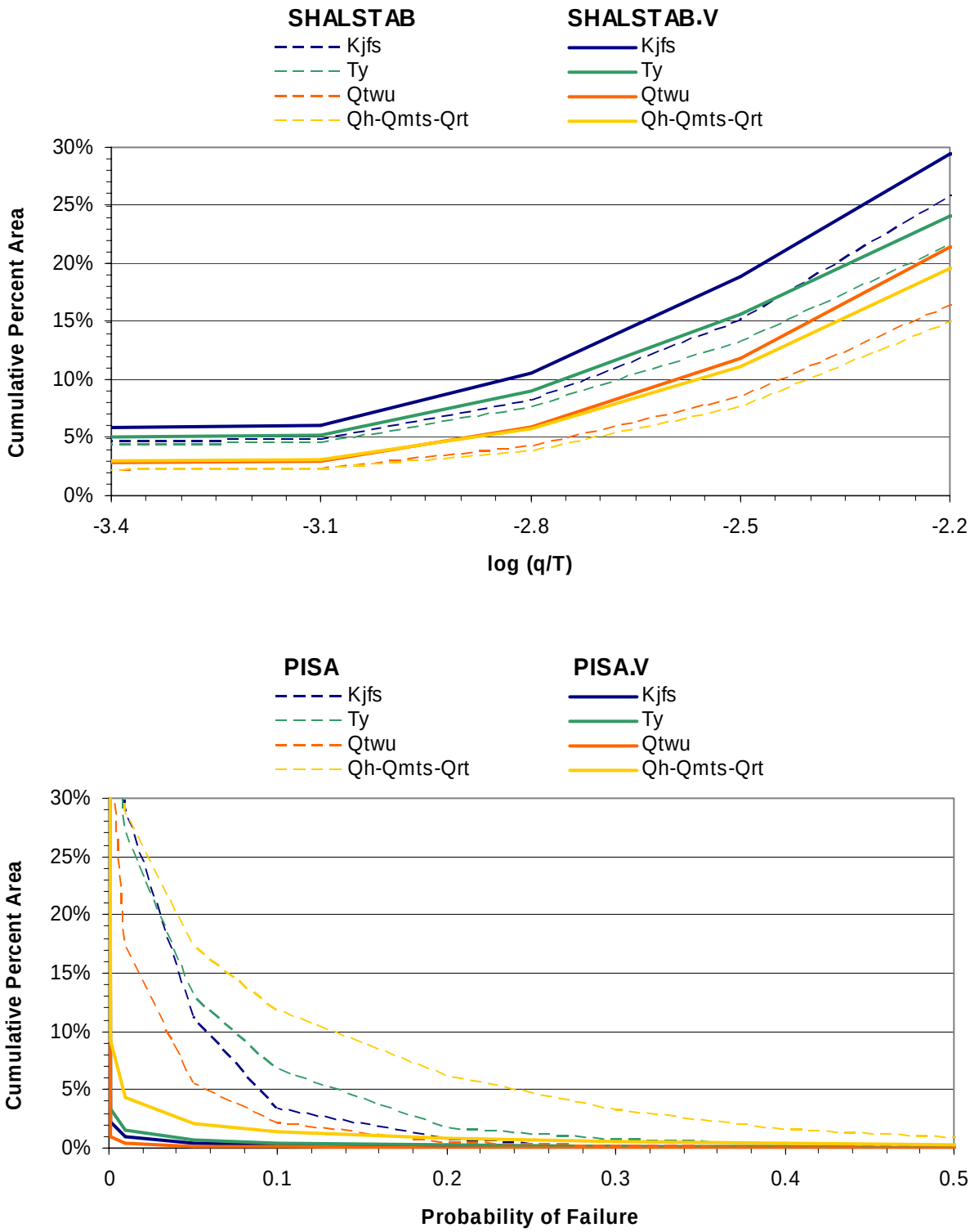

Figure 3-9. Cumulative percent of watershed area in instability classes: a) SHALSTAB and SHALSTAB.V, b) PISA and PISA.V.

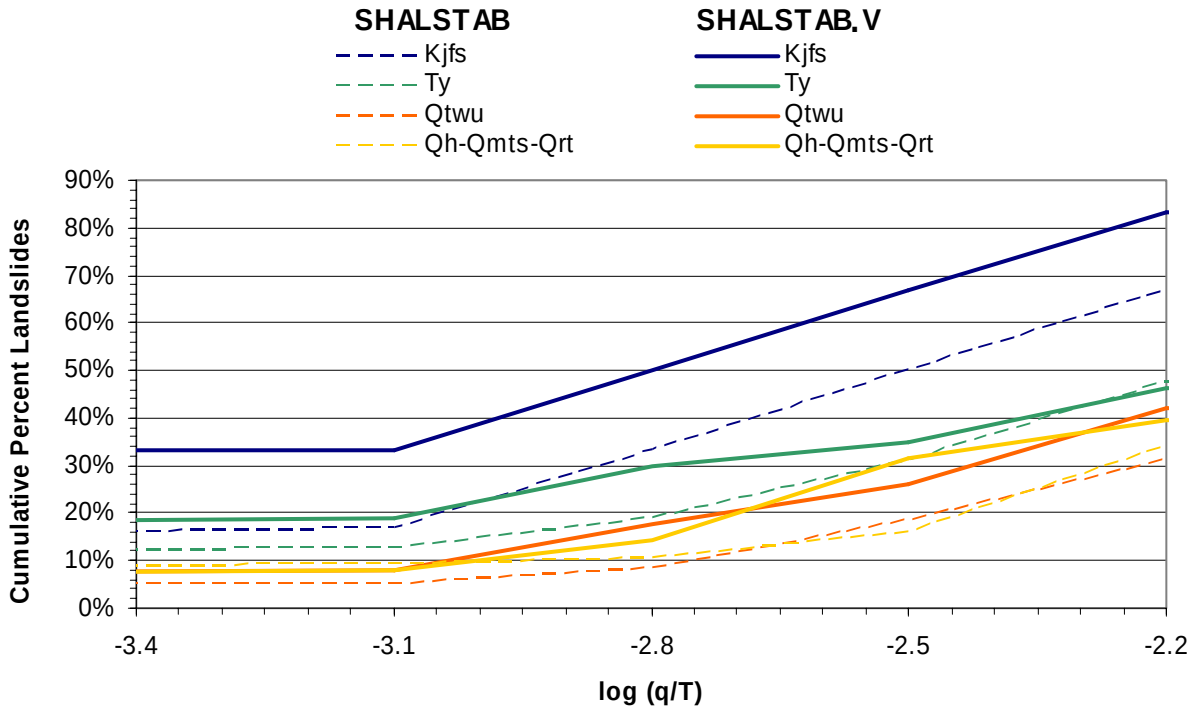

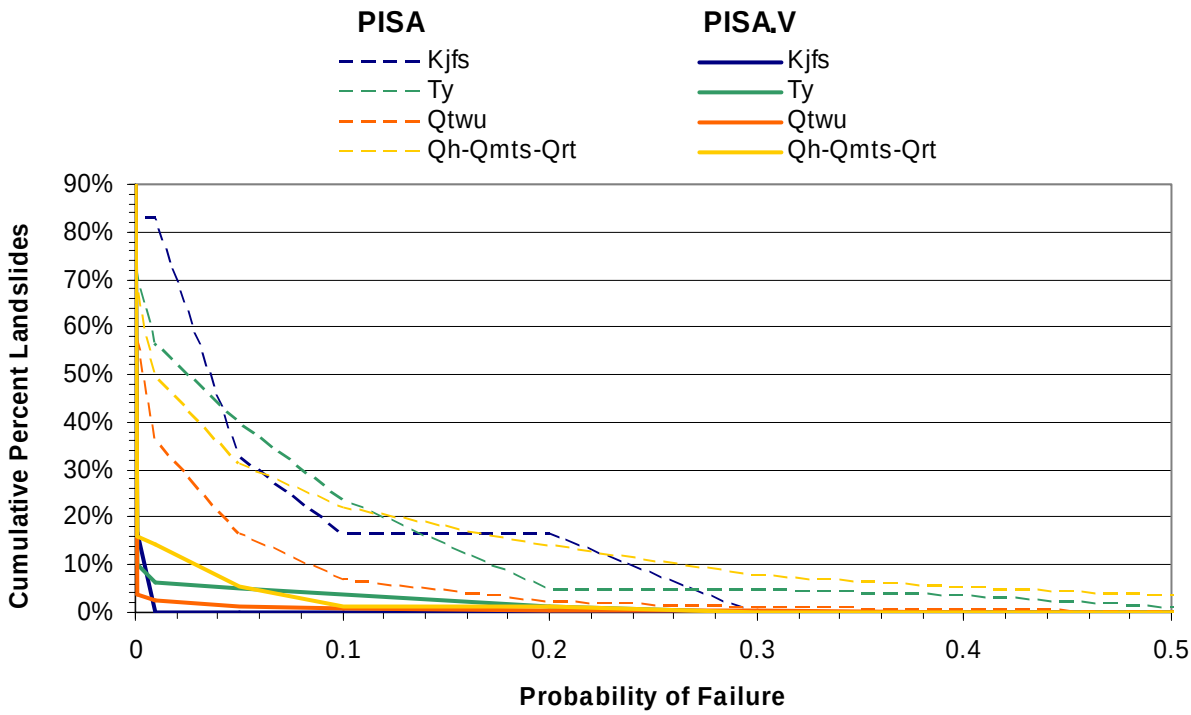

Figure 3-10. Cumulative percent of landslides in instability classes: a) SHALSTAB and SHALSTAB.V, b) PISA and PISA.V.

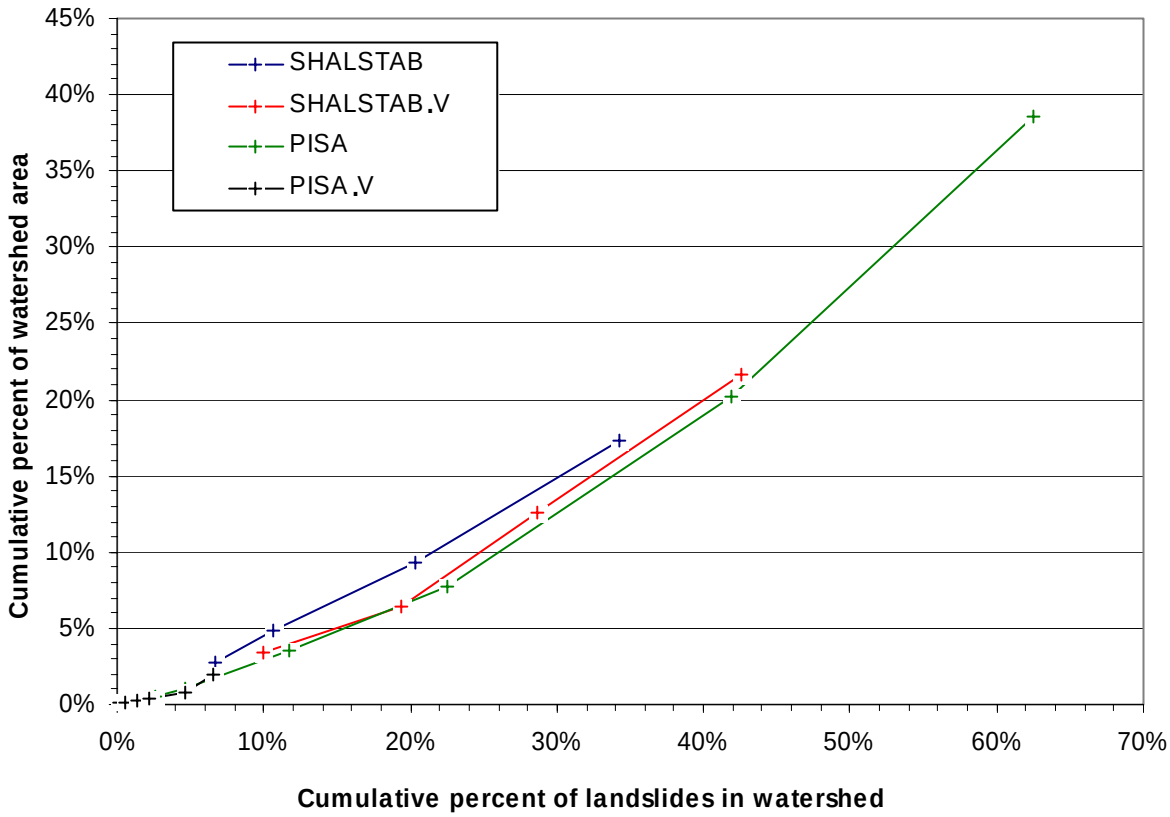

Figure 3-11. Cumulative percent of watershed area as a function of the cumulative percent of the number of landslides.

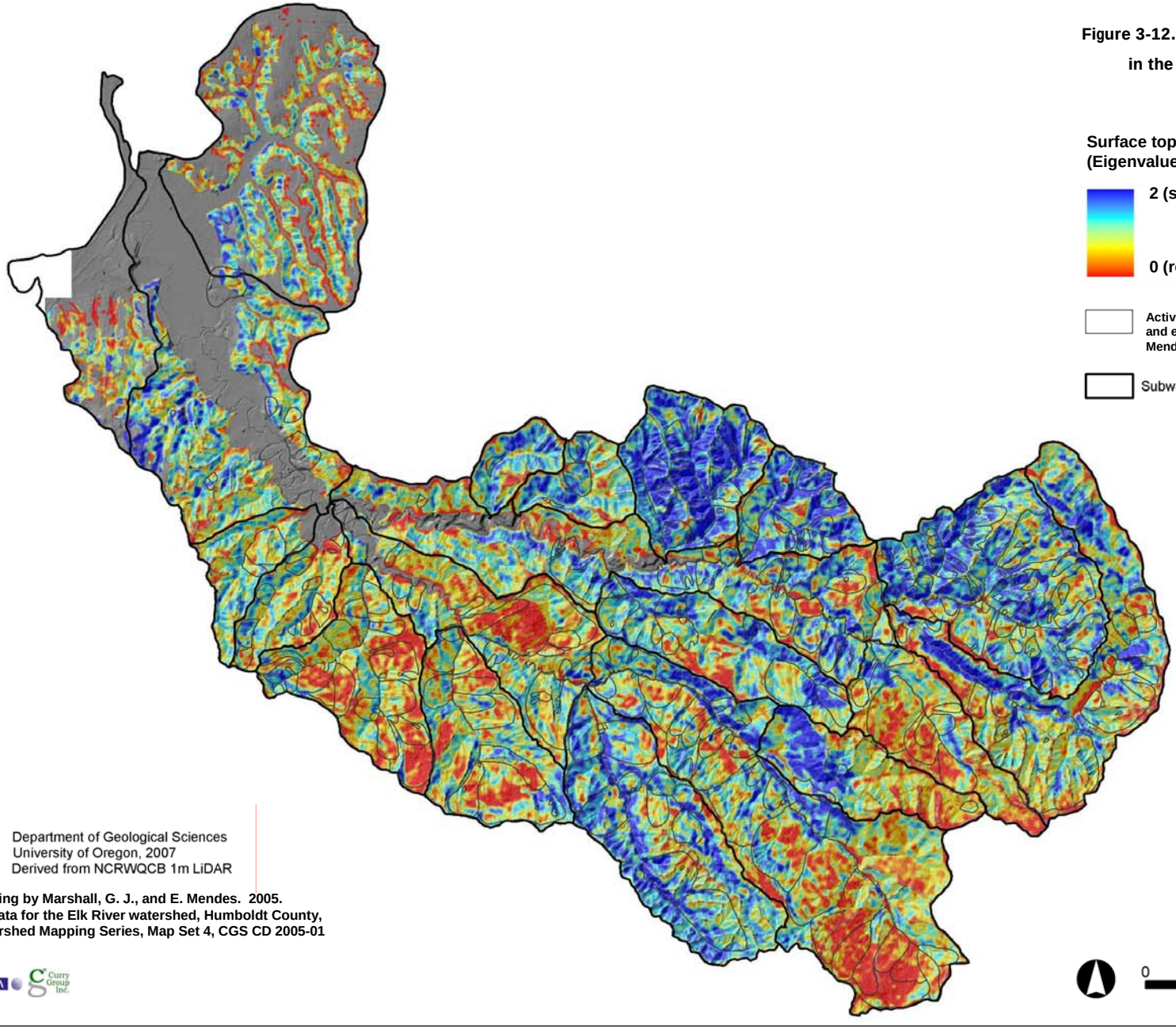

Figure 3-12. DSLED-Rough results in the Elk River basin.

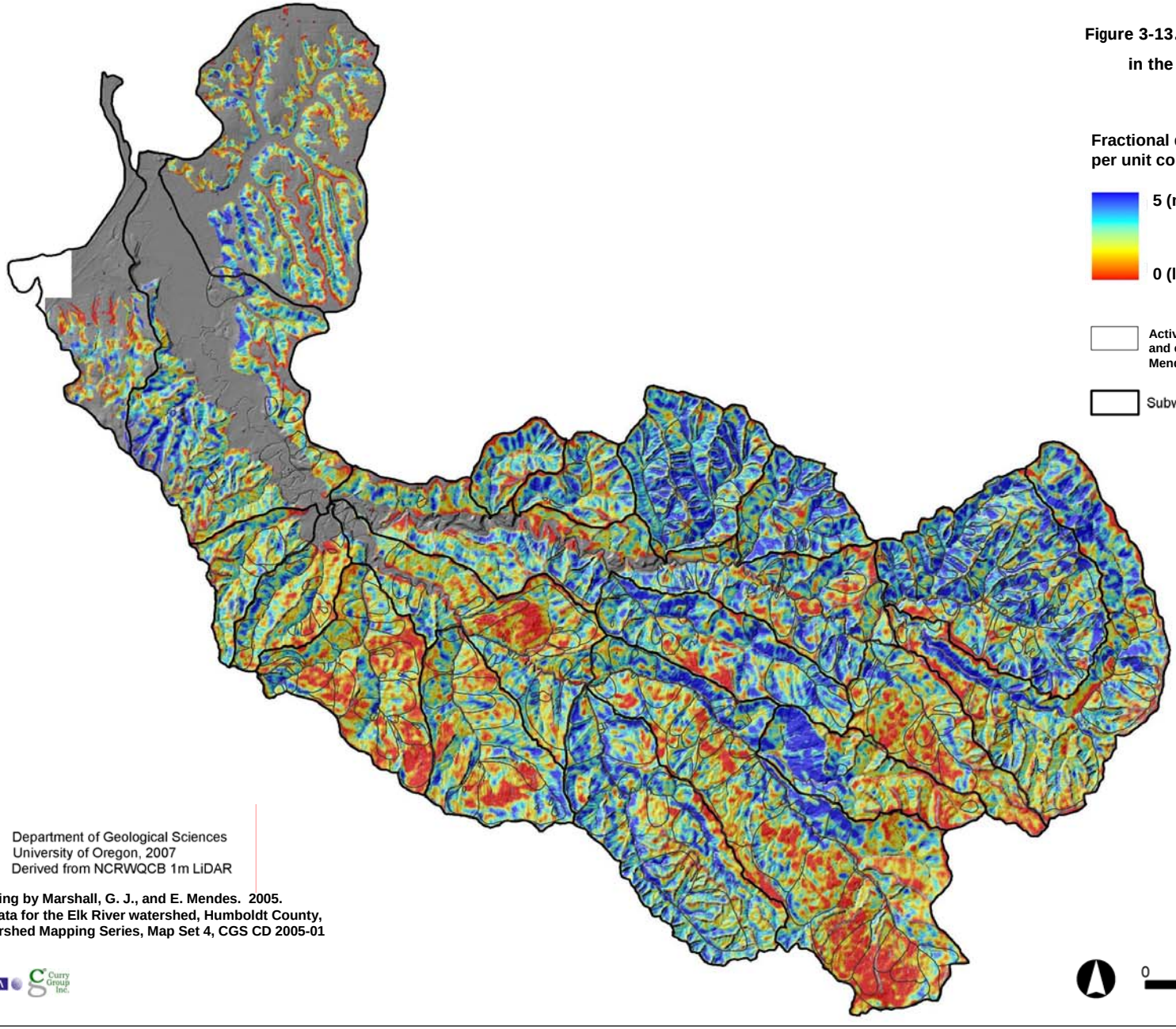

Figure 3-13. DSLED-Drain results in the Elk River basin.

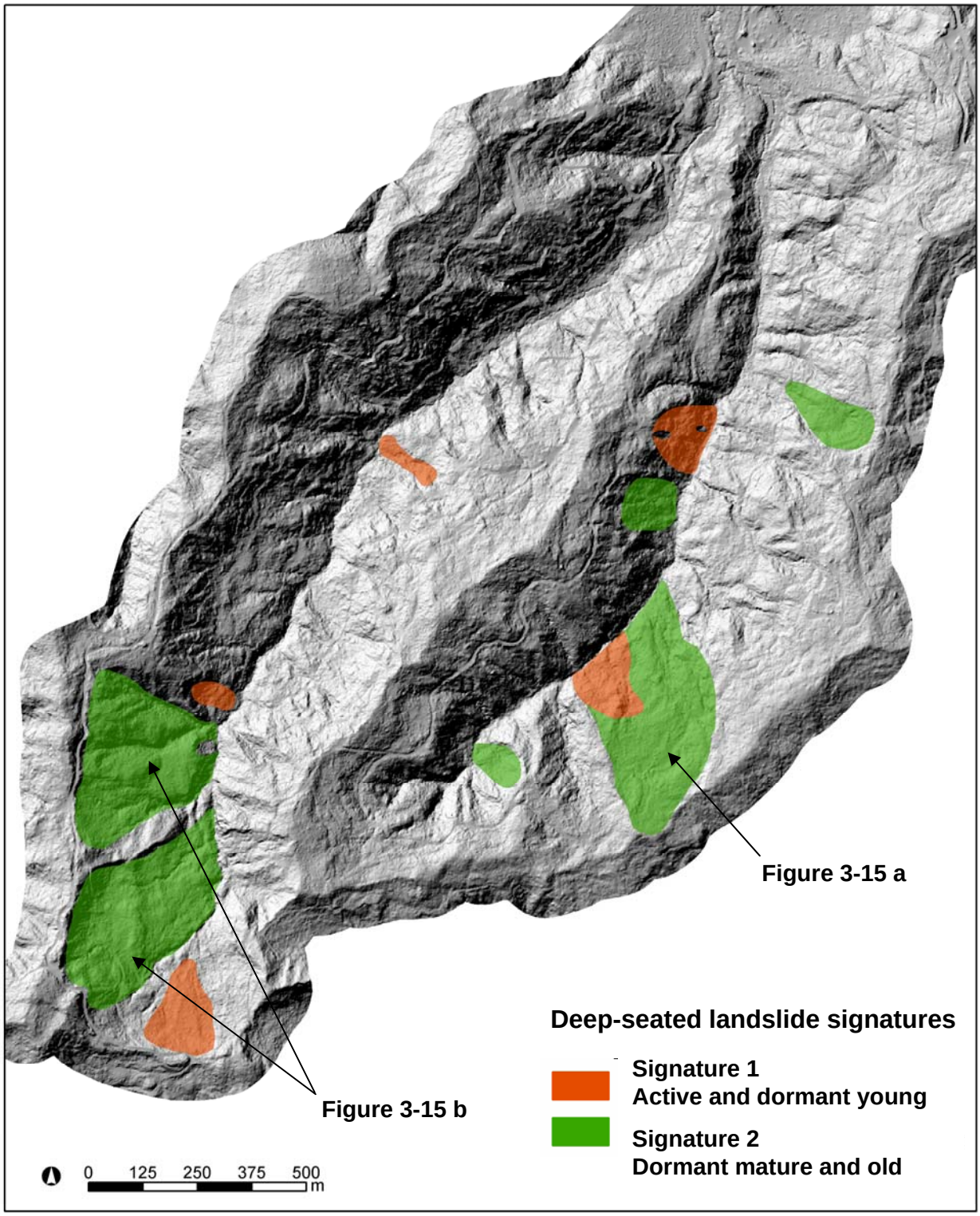

Figure 3-14. Deep-seated landslide signatures in Railroad Gulch.

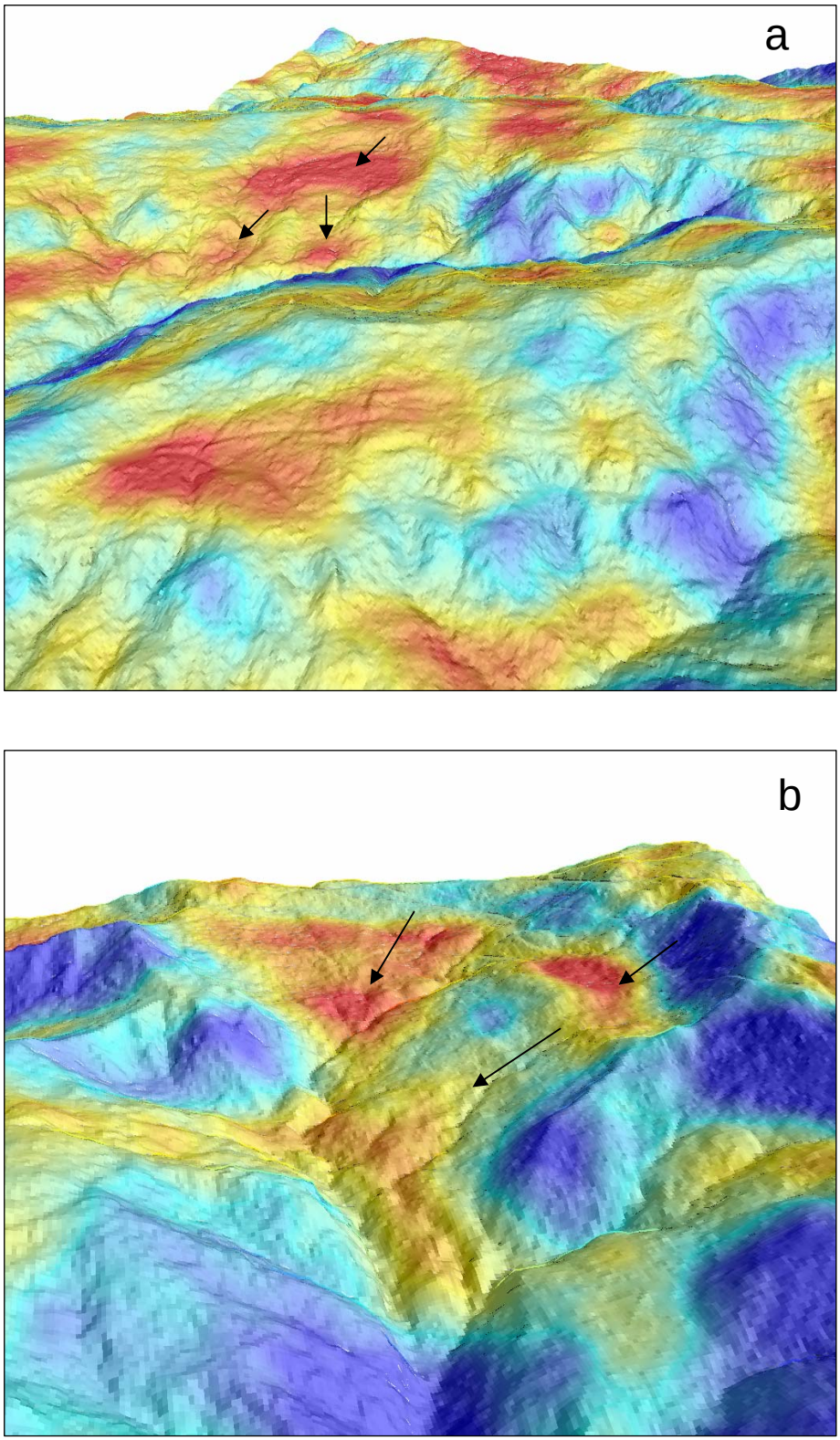

Figure 3-15. DSLED-Rough results in the vicinity of mapped deep-seated landslides in Railroad Gulch.

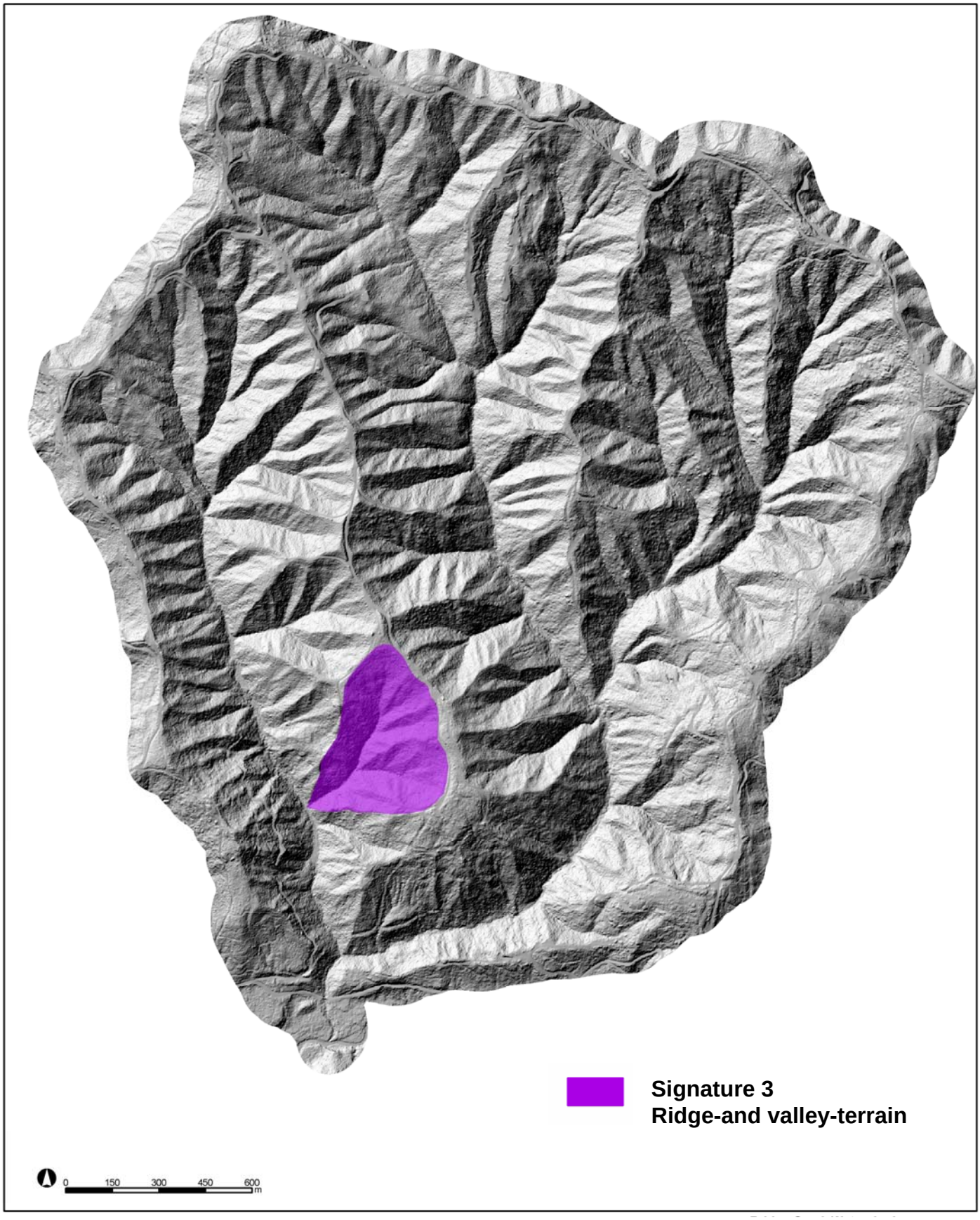

Figure 3-16. Signature of ridge-and-valley topography in Bridge Creek.